NASA CS-72346

EVALUATION OF LUBRICANTS FOR HIGH-SPEED HIGH-TEMPERATURE APPLICATIONS

by

J. W. Kannel, J. C. Bell,
R. R. Riopelle, and C. M. Allen

Prepared for

NATIONAL AERONAUTICS AND SPACE ADMINISTRATION

CONTRACT NAS 3-7270, Task Order No. 2

BATTELLE MEMORIAL INSTITUTE

COLUMBUS LABORATORIES

NOTICE

This report was prepared as an account of Government sponsored work. Neither the United States, nor the National Aeronautics and Space Administration (NASA), nor any person acting on behalf of NASA:

A.) Makes any warranty or representation, expressed or implied, with respect to the accuracy, completeness, or usefulness of the information contained in this report, or that the use of any information, apparatus, method, or process disclosed in this report may not infringe privately owned rights; or

B.) Assumes any liabilities with respect to the use of, or for damages resulting from the use of any information, apparatus, method or process disclosed in this report.

As used above, "person acting on behalf of NASA" includes any employee or contractor of NASA, or employee of such contractor, to the extent that such employee or contractor of NASA, or employee of such contractor prepares, disseminates, or provides access to, any information pursuant to his employment or contract with NASA, or his employment with such contractor.

Requests for copies of this report should be referred to:

National Aeronautics and Space Administration
Scientific and Technical Information Division
Attention: USS-A
Washington, D. C. 20546

NASA CR-72346

FIRST SUMMARY REPORT

on

EVALUATION OF LUBRICANTS FOR HIGH-SPEED HIGH-TEMPERATURE APPLICATIONS

by

J. W. Kannel, J. C. Bell,
R. R. Riopelle, and C. M. Allen

Prepared for

NATIONAL AERONAUTICS AND SPACE ADMINISTRATION

November, 1967

Contract NAS 3-7270, Task Order No. 2

Technical Management
NASA Lewis Research Center
Cleveland, Ohio
D. P. Townsend, Project Manager
E. V. Zaretsky, Research Advisor

BATTELLE MEMORIAL INSTITUTE
Columbus Laboratories
505 King Avenue
Columbus, Ohio 43201

ABSTRACT

Research has been conducted to determine the feasibility of using a rolling-disk apparatus to evaluate lubricants for high-speed, high-temperature applications such as the SST. The instrumentation to be used with the apparatus includes an X-ray technique for measuring the thickness of the lubricant film between the disks and a dielectric breakdown scheme for detecting surface-to-surface contact. A detailed study has been conducted to define a disk geometry which best simulates the contact geometry of a 120 mm bore angular-contact ball bearing. From the results of this study, it was determined that the disks should be 1.4 inches in diameter and have a crown radius of 11 inches. Both cylindrical-crowned disks and coned-crowned disks should be used, the latter to simulate sliding conditions due to ball spin. Cylindrical-crowned disks of M-50 bearing steel have been fabricated. Check-out experiments have demonstrated the basic capability of the disk machine to duplicate the required operating conditions. Preliminary exploratory experiments with the similitude disk have indicated that only a very thin lubricant film is formed between bearing elements at temperatures around 600 F, under moderate loads and speeds, when the fluid designated XRM-177 is utilized. At a milder temperature, 400 F, films between 3 and 8 microinches are formed.

TABLE OF CONTENTS

TABLE OF CONTENTS (Continued)

LIST OF FIGURES

APPENDIX

LIST OF TABLES

EVALUATION OF LUBRICANTS FOR HIGH-SPEED HIGH-TEMPERATURE APPLICATIONS

by

J. W. Kannel, J. C. Bell, R. R. Riopelle, and C. M. Allen

INTRODUCTION

Advanced air-breathing propulsion systems, such as the engines for the supersonic transport, will operate at speeds, power levels, and temperatures which are significantly higher than in present systems. The selection of a fluid which will adequately lubricate the mainshaft engine bearings to obtain the necessary time between overhauls will require careful analysis and extensive evaluation.

The lubrication and failure mechanisms in rolling-element bearings are complex and not fully understood. As a result, the evaluation of bearing designs and lubricants requires that a statistically significant number of bearings must be run to failure in candidate fluids under the projected conditions of operation and environment. NASA has recently supported such an evaluation study for candidate supersonic-transport bearings and lubricants. In general, full-scale bearing fatigue studies involve the expenditure of considerable time, effort, and money to obtain meaningful results because of the degree of scatter typically found in bearing fatigue data. In addition, the data obtained do not readily lend themselves to extrapolation to fluids or operating conditions other than those used in the tests. This limitation arises, at least partially, from the fact that the full-scale bearing approach is inherently unable to yield much fundamental information regarding the process of lubrication in rolling contacts.

In the past few years, significant progress has been made in evaluating and understanding the elastohydrodynamic-lubrication phenomenon in rolling-element

mechanisms. At Battelle, experimental techniques have been developed to measure actual lubricant film-thickness profiles (and consequently, surface deformation profiles) and surface pressures and temperatures in the contact region between rolling/sliding disks which simulate the contact of ball bearings*. Electrical continuity measurements have also been devised which indicate the extent of full-fluid-film lubrication between the disks. These techniques, together with associated theoretical analyses, have resulted in an improved understanding of the elastohydrodynamic lubrication process in rolling contacts.

The purpose of the present research program is to apply these experimental techniques, together with the improved understanding of elastohydrodynamic lubrication, to the lubrication of mainshaft engine bearings for the supersonic transport. The studies are to be conducted with a rolling-disk machine using disks that accurately simulate the dynamic situation of a ball-race contact in a bearing. The extent of elastohydrodynamic lubrication will be determined over the range of anticipated operating conditions, for disks simulating the contact of mainshaft bearings. These data will be correlated with data from full-scale bearing studies being conducted elsewhere to yield the relation between extent of elastohydrodynamic lubrication and failure. These studies should make it possible to select the best combination of lubricant and bearing material for a much wider set of operating parameters than would be possible using full-scale bearing tests alone.

The specific objective of Task II of the study has been to find disk geometry, to get accurate simulation of candidate supersonic transport bearings, and to conduct check-out and exploratory film-thickness experiments with these disks.

---

* The research leading to these techniques was sponsored by the USAF through the Research and Technology Division, Wright-Patterson Air Force Base, Ohio. For example, see References 1 and 2.

DESIGN OF DISKS TO BE USED IN LUBRICATION STUDY

The Ball Bearing to be Simulated

The ball bearing being evaluated by the NASA Lewis Research Center in rolling-element fatigue has a 120 mm bore and contains fifteen 13/16-inch-diameter balls moving in a path having a pitch diameter of 6.1023 in. The conformity between the balls and races is such that the undeformed transverse radius is 0.52 times the ball diameter for the outer race and 0.54 for the inner race. The initial contact angle is 20 degrees, that is, if the load is very light the line from the center of the ball to the center of either contact area is tilted 20 degrees with respect to the line from the bearing center to the ball center. Both the balls and races are made of steel having Young's modulus 29 x 10^6 lb/in.^{2} and Poisson's ratio 0.25.

Two operating conditions will be considered in the simulation study, one having a thrust load of 3290 pounds with the outer race turning at 12,500 rpm, the other having a thrust load of 5,800 pounds with the inner race turning at 12,500 rpm*. Centrifugal force, of course, also adds to the loads and makes the operating contact angles different on the two races. The general situation of one ball between the two races is then as shown in Figure 1, which also illustrates some notation to be used.

The contact forces (W_i and W_o), contact angles (β_i and β_o), semiaxes of both Hertzian (dry) contact areas, and various angular speeds for each ball have been computed for both sets of operating conditions by the General Electric Company[3,4] using the Rolling Element Computer Analysis Program (RECAP),

---

* The speed of 12,500 spin was a target condition used in References 3 and 4, though later bearing tests used speeds only up to 12,000 rpm. An intermediate load also was used in place of the lighter load presumed here (yielding maximum Hertz pressure of 295,000 psi instead of 269,000 psi).[5]

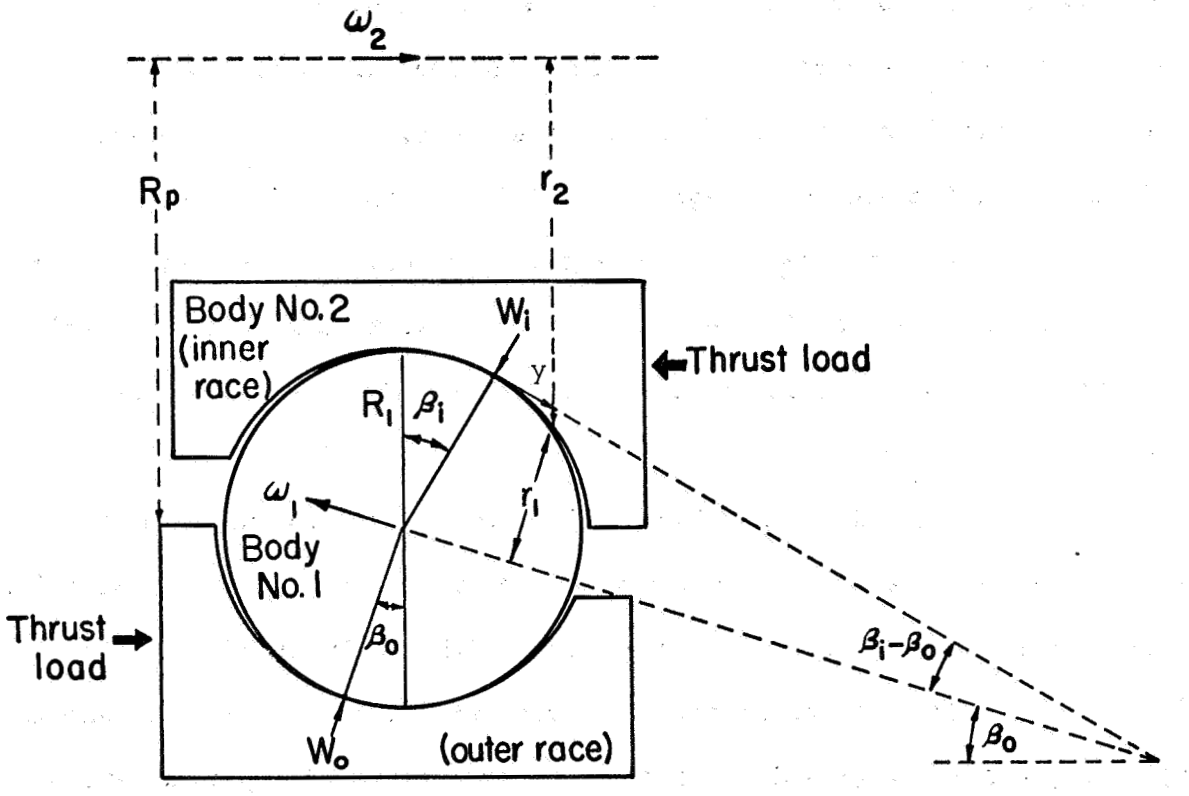

FIGURE 1. GEOMETRY OF THE BALL-RACE CONTACT

constructed by A. B. Jones. Ball control in each case is maintained by the outer race, so that the balls spin with respect to the inner race but not the outer. Since the experiments now being planned are to consider the effects of ball spin on lubrication, it is the contact between the ball and the inner race which should be simulated. Therefore, several parameters have been collected in Table 1 describing the contact between the ball (Body No. 1) and the inner race (Body No. 2). These parameters were derived as indicated in the table, from either the bearing specifications, or from the theory of Hertzian (dry) contact[6], or from the RECAP calculations taking Ball No. 1 as being representative. In this table, R_1 and R_1' are the principle radii of the undeformed ball at contact, R_2 and R_2' are those of the inner race, R_p is pitch radius, E_1 and E_2 are Young's moduli, ν_1 and ν_2 are Poisson ratios, x_h and y_h are semiaxes of Hertz contact in the rolling and axial directions, p_h is maximum Hertz pressure, and ω_1 and ω_2 are angular velocities of the surfaces passing the contact area. It is interesting to note that the quantities x_h, y_h, and p_h computed for this table (partly independently from the RECAP) agree with those obtained from the RECAP calculations to within small differences in their fifth digits.

The bearing parameters of interest in the experimental simulation process are R, R′, W, E′, and the rolling velocities u_1 and u_2 of the two surfaces. In view of the ball spin and the Heathcote slip, these two velocities vary with the lateral distance y from the center of the contact area. In view of Figure 1,

$$u_1(y) = \omega_1 r_1(y), \qquad u_2(y) = \omega_2 r_2(y) \quad .$$

Evaluating the variations of $r_1(y)$ and $r_2(y)$ geometrically, taking the curvature of the interface to be the average of the underformed curvatures of the surfaces, one finds

TABLE 1. GEOMETRICAL AND PHYSICAL PARAMETERS OF THE BALL-RACE CONTACT

Parameter	Case 1 Values[a]	Case 2 Values[b]	Source
β_i, deg	26.855	27.495	RECAP
β_o, deg	18.407	20.453	RECAP
R_1 or R_1', inch	0.40625	0.40625	design
R_2, inch	3.01375	3.03341	$R_2 = R_p \sec \beta_i - R_1$
R_2', inch	-0.43875	-0.43875	design
R, inch	0.35799	0.35827	$R = 1/(\frac{1}{R_1} + \frac{1}{R_2})$
R', inch	5.48438	5.48438	$R' = 1/(\frac{1}{R_1'} + \frac{1}{R_2'})$
R'/R	15.3199	15.3080	ratio
k (= x_h/y_h)	0.17018	0.17026	Eq. (52) of Ref. 6[c]
m	0.48281	0.48289	Eq. (54) of Ref. 6[d]
n	2.83701	2.83617	m = kn
W, lb	489.04	841.04 lb	RECAP[e] inner race load
E', lb/inch^2	48.590×10^6	48.590×10^6	$E' = 1/(\frac{1-\nu_1^2}{\pi E_1} + \frac{1-\nu_2^2}{\pi E_2})$
$W/(E'R^2)$	78.533×10^{-6}	134.851×10^{-6}	ratio
Δ	0.070298	0.084179	$\Delta = [\frac{3\pi W R'}{2E'R^2(R+R')}]^{1/3}$
$R\Delta$, inch	0.025166	0.030159	product
x_h, inch	0.012151	0.014563	$x_h = mR\Delta$
y_h, inch	0.071397	0.085535	$y_h = nR\Delta$
$\sqrt{x_h y_h}$, inch	0.029453	0.035294	product
p_h, lb/inch^2	269163	322370	$p_h = \frac{E'\Delta}{\pi^2 mn}(1 + \frac{R}{R'})$
ω_1, rpm	46891	46790	RECAP rotational velocity
ω_2, rpm	6962.2	6967.1 (= 12500-5532.9)	RECAP orbital velocity

(a) Case 1 has a thrust load of 3290 lb and the outer race rotating at 12500 rpm.
(b) Case 2 has a thrust load of 5800 lb and the inner race rotating at 12500 rpm.
(c) The equation is $\frac{(1/k^2)E(k')-K(k')}{K(k')-E(k')} = \frac{R'}{R}$, where K(k') and E(k') are complete elliptic integrals and $k'^2 = 1 - k^2$.
(d) The equation implies that $m = \sqrt[3]{\frac{2}{\pi} kE(k')}$.
(e) $W = \frac{2\pi}{3} x_h y_h p_h = \pi \bar{W} x_h y_h$, and RECAP computes x_h, y_h, and $\bar{W}$ (the mean compressive stress).

$$u_1(y) = \omega_1[R_1 \cos(\beta_i \beta_o) - y \sin(\beta_i - \beta_o) - \frac{y^2}{4}(\frac{1}{R_1'} - \frac{1}{R_2'}) \cos(\beta_i - \beta_o)] ,$$

$$u_2(y) = \omega_2[R_p - R_1 \cos\beta_i + y \sin\beta_i + \frac{y^2}{4}(\frac{1}{R_1'} - \frac{1}{R_2'}) \cos\beta_i] .$$

If we denote $R_2' = -(1+\varepsilon) R_1'$, so that $(1+\varepsilon)/2$ is the usual measure of conformity between the ball and race, and note that $R_1' = R_1$, then $\frac{1}{R_1'} - \frac{1}{R_2'} = \frac{2+\varepsilon}{R_1(1+\varepsilon)}$.

Note also the $R_2 = R_p \sec\beta_i - R_1$ to within the necessary accuracy. Using the parameters shown in Table 1, it follows that

$$u_1(y) = 1973.2 - 721.4\, y - 5756.6\, y^2 ,$$

$$u_2(y) = 1960.3 + 329.4\, y + 770.9\, y^2 ,$$

for y in inches and u in in/sec, and for Case 2 that

$$u_1(y) = 1975.5 - 600.7\, y - 5763.4\, y^2 ,$$

$$u_2(y) = 1963.2 + 336.8\, y + 767.0\, y^2 ,$$

The range of variation of these velocities is shown in Table 2. Values of $u_1 + u_2$ and $u_2 - u_1$ are included since these are important quantities in isothermal lubrication and heat generation, respectively. The other parameters that must be taken into account in the simulation process are those of the lubricant viscosity. For isothermal lubricant, the viscosity can be taken to be

$$\mu = \mu_o e^{\gamma p} ,$$

where p is the local pressure in the lubricant, so that the base viscosity μ_o and the pressure viscosity coefficient γ must be considered too.

Geometry of the Rolling Disks

For experimental purposes, the contact between the rolling ball and race is to be represented by a contact between two disks rolling together on their lateral surfaces. In order to get sufficient adaptability in the disk design, the disks may be allowed to have lateral surfaces that are either convexly or

TABLE 2. REPRESENTATIVE SURFACE VELOCITIES FOR THE BALL-RACE CONTACT

Case	y, in.	u_1, in./sec	u_2, in./sec	$u_1 + u_2$, in./sec	$u_2 - u_1$, in./sec
I	-0.071397 (= $-y_h$)	1995.4	1940.7	3971.5	- 54.7
	0.000000	1973.2	1960.3	3933.5	- 12.9
	+0.071397 (= $+y_h$)	1892.4	1987.7	3915.5	+ 95.3
II	-0.085531 (= $-y_h$)	1984.7	1940.0	3975.2	- 44.7
	0.000000	1975.5	1963.2	3938.7	- 12.3
	+0.085531 (= $+y_h$)	1881.9	1997.6	3930.0	+115.7

concavely toroidal, and the axes of rotation of the disks may be tilted with respect to each other. The general configuration of such a system is shown in Figure 2, which also illustrates some of the notation to be used. It should be noted that the notation here includes a bar over each letter, the bar indicating that this symbol refers to a parameter of the experimental model. (Parameters for the prototype bearing are unbarred.) In drawing the rolling disks, the axis of the upper disk (representing the inner race) has been tilted instead of that of the lower disk (representing the ball), since the axis of the upper disk is more easily skewed in the actual disk machine, so in effect Figure 2 is tilted counterclockwise from Figure 1 by an angle β_o.

Considering that the deformed radius of lateral curvature of the contact area is $\frac{1}{2}(\bar{R}_1' - \bar{R}_2')$, the radii of rotation of points on the rolling surfaces at lateral distance $\bar{y}$ from the center of contact are

$$\bar{r}_1(\bar{y}) = \bar{r}_{1c} - \bar{y}\sin\bar{\beta}_c - \frac{\bar{y}^2}{4}\left(\frac{1}{\bar{R}_1'} - \frac{1}{\bar{R}_2'}\right)\cos\bar{\beta}_c \quad ,$$

$$\bar{r}_2(\bar{y}) = \bar{r}_{2c} + \bar{y}\sin(\bar{\beta}_t + \bar{\beta}_c) + \frac{\bar{y}^2}{4}\left(\frac{1}{\bar{R}_1'} - \frac{1}{\bar{R}_2'}\right)\cos(\bar{\beta}_t + \bar{\beta}_c) \quad .$$

Here $\bar{r}_{1c}$ and $\bar{r}_{2c}$ represent the disk radii measured to the centers of contact, but the principal radii of the undeformed surfaces there are denoted as $\bar{R}_1$ and $\bar{R}_2$ in the rolling direction and $\bar{R}_1'$ and $\bar{R}_2'$ in the lateral direction. It may be observed that the tilt angle $\bar{\beta}_t$ corresponds to the contact angle β_o in the ball bearing, and $\bar{\beta}_c$ (the cone angle) corresponds to $\beta_i - \beta_o$, though for the sake of generality, these pairs of corresponding angles will not be assumed equal until that becomes necessary. From geometrical considerations,

$$\bar{r}_{1c} = \bar{R}_1\cos\bar{\beta}_c, \quad \text{and } \bar{r}_{2c} = \bar{R}_2\cos(\bar{\beta}_t + \bar{\beta}_c) \quad .$$

Letting $\bar{\omega}_1$ and $\bar{\omega}_2$ be the angular velocities of the disks, their surface velocities

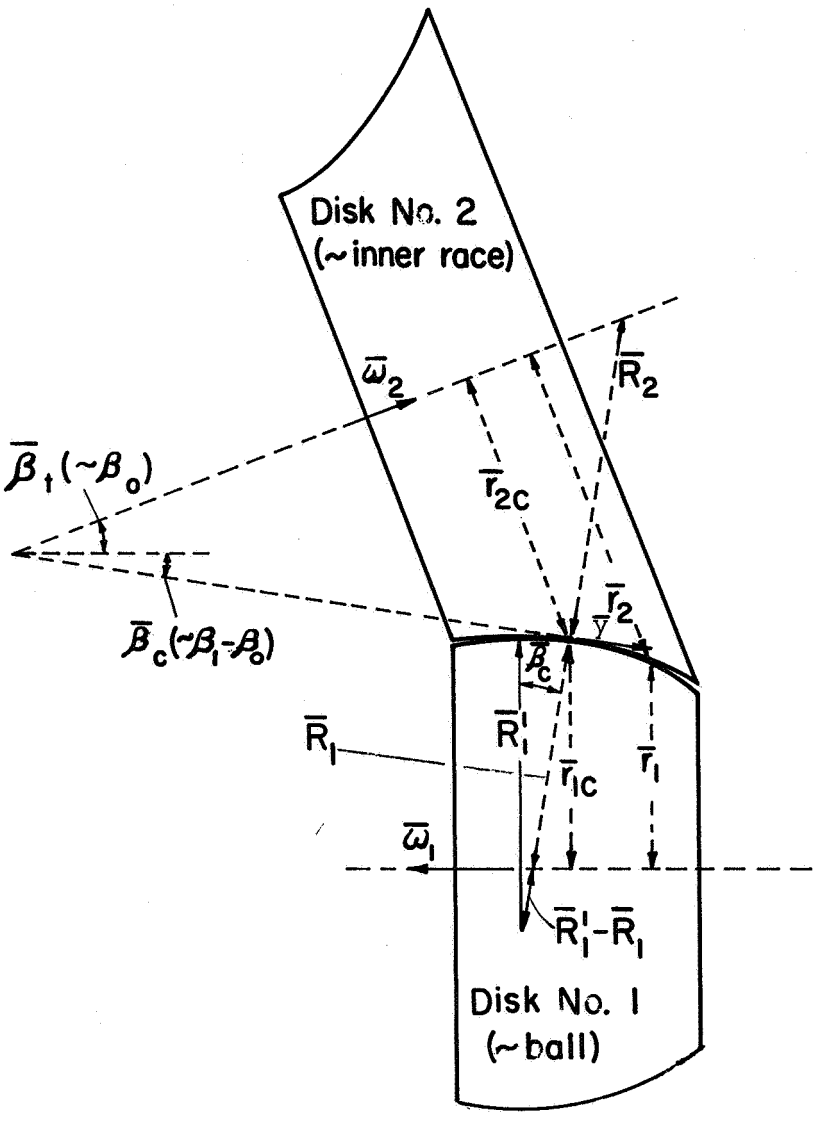

FIGURE 2. GEOMETRY OF CONTACT OF TWO ROLLING DISKS

at lateral distance $\bar{y}$ from the center of contact become

$$\bar{u}_1(\bar{y}) = \bar{\omega}_1[\bar{R}_1 \cos \bar{\beta}_c - \bar{y} \sin \bar{\beta}_c - \frac{\bar{y}^2}{4} (\frac{1}{\bar{R}'_1} - \frac{1}{\bar{R}'_2}) \cos \bar{\beta}_c] \quad ,$$

$$\bar{u}_2(\bar{y}) = \bar{\omega}_2[\bar{R}_2 \cos(\bar{\beta}_t + \bar{\beta}_c) + \bar{y} \sin(\bar{\beta}_t + \bar{\beta}_c) + \frac{\bar{y}^2}{4} (\frac{1}{\bar{R}'_1} - \frac{1}{\bar{R}'_2}) \cos(\bar{\beta}_t + \bar{\beta}_c)] \quad .$$

These velocities, together with the design radii of the disks and the load $\bar{W}$ and the reduced elastic modulus $\bar{E}'$, define the geometrical and mechanical aspects of the disk contact relevant to the simulation of ball-race contact.

The dimensions of dry contact between the disks may be found by the procedure outlined in Table 1. In particular, let

$$\bar{R} = 1/(\frac{1}{\bar{R}_1} + \frac{1}{\bar{R}_2}) \quad , \qquad \bar{R}' = 1/(\frac{1}{\bar{R}'_1} + \frac{1}{\bar{R}'_2}) \quad ,$$

$$\bar{\Delta} = [\frac{3\pi \bar{W} \bar{R}'}{2\bar{E}'\bar{R}^2(\bar{R} + \bar{R}')}]^{1/3} \quad , \qquad \text{where } \frac{1}{\bar{E}'} = \frac{1-\bar{\nu}_1^2}{\pi \bar{E}_1} + \frac{1-\bar{\nu}_2^2}{\pi \bar{E}_2} \quad ,$$

and let $\bar{k}$ be the solution of

$$\frac{(1/\bar{k}^2) E(\bar{k}') - K(\bar{k}')}{K(\bar{k}') - E(\bar{k}')} = \frac{\bar{R}'}{\bar{R}} \quad ,$$

where $K(\bar{k}')$ and $E(\bar{k}')$ are complete elliptic integrals of the first and second kinds and $\bar{k}'^2 = 1 - \bar{k}^2$. Also let

$$\bar{m} = \sqrt[3]{\frac{2}{\pi} \bar{k} E(\bar{k}')} \quad , \qquad \bar{n} = \bar{m}/\bar{k} \quad .$$

Then the semiaxes $\bar{x}_h$ and $\bar{y}_h$ of dry contact and its maximum pressure $\bar{p}_h$ are

$$\bar{x}_h = \bar{m} \bar{R} \bar{\Delta} \quad , \quad \bar{y}_h = \bar{n} \bar{R} \bar{\Delta} \quad , \quad \text{and } \bar{p}_h = \frac{\bar{E}'\bar{\Delta}}{\pi \bar{m} \bar{n}} (1 + \frac{\bar{R}}{\bar{R}'}) \quad .$$

Selection of Conditions for Experimental Similitude

The requirements for similitude in lubrication processes between the ball-race system and the rolling-disk system are discussed in Appendix A. In describing the results found there, one may let λ represent the ratio of the relative radius $\bar{R}$ of curvature in the rolling direction in the rolling-disk system and the corresponding radius R in the ball-race system, that is

$$\lambda = \bar{R}/R \quad .$$

Then for similarity in cases where the lubricant can be treated as being isothermal, it is required that the radii of curvature in the transverse direction (R' and $\bar{R}'$), the total loads (W and $\bar{W}$) and the surface velocities [$u_1(y)$, $u_2(y)$, and $\bar{u}_1(\bar{y})$, $\bar{u}_2(\bar{y})$] at lateral distance y or $\bar{y}$ (which corresponds to λy) from the center of contact should share the relationships

$$\bar{R}' = \lambda R' \quad ,$$

$$\bar{W} = \lambda^2 W \quad ,$$

$$\bar{u}_1(\lambda y) + \bar{u}_2(\lambda y) = \lambda \, [u_1(y) + u_2(y)] \quad .$$

(It is assumed here that the same lubricant and bearing materials are used in both systems--if the materials were changed these relationships would change.) If local temperature variations in the lubricant affect the lubrication processes significantly then it is necessary to add the restriction

$$\bar{u}_2(\lambda y) - \bar{u}_1(\lambda y) = \lambda \, [u_2(y) - u_1(y)] \quad ,$$

and, in fact, to require that $\lambda = 1$. (The parameter λ will still be shown even for the thermal case, so that its role may be identified in case it is not possible to satisfy completely the requirement that $\lambda = 1$.) These requirements for similitude can prove to be quite stringent, so we will consider how they may be met at various levels of exactitude. In all these cases we will include at least some consideration of the thermal effects, since the distinctive feature of the

present research is that it includes the effect of variable slip between the surfaces, and this slip is important only if thermal effects are significant.

Ideal Simulation

Suppose an effort is to be made to satisfy all the requirements for lubrication similitude that have just been stated. These imply

$$\bar{R} = \lambda R, \qquad \bar{R}' = \lambda R',$$

$$\bar{u}_1(\lambda y) \equiv \lambda u_1(y), \qquad \bar{u}_2(\lambda y) \equiv \lambda(y),$$

$$\bar{W} = \lambda^2 W, \qquad \lambda = 1.$$

The requirement on load W stands somewhat apart from the others, so long as the disk machine is simply strong enough to accept any desired load, and the condition that $\lambda = 1$ should perhaps be deferred during early consideration, but the remaining four requirements intertwine in their demands on the experimental design, so their implications need examination. Considering the definitions of the relative radii of curvature and the quadratic functions of y that were found for the surface velocities, these four requirements demand that

$$\left.\begin{aligned}
&\frac{\lambda}{\bar{R}_1} + \frac{\lambda}{\bar{R}_2} = \frac{1}{R_1} + \frac{1}{R_2} \quad , \\
&\frac{\lambda}{\bar{R}'_1} + \frac{\lambda}{\bar{R}'_2} = \frac{1}{R'_1} + \frac{1}{R'_2} \quad , \\
&\bar{\omega}_1 \bar{R}_1 \cos \bar{\beta}_c = \lambda\, \omega_1 R_1 \cos(\beta_i - \beta_o) \quad , \\
&\bar{\omega}_1 \sin \bar{\beta}_c = \omega_1 \sin(\beta_i - \beta_o) \quad , \\
&\frac{\bar{\omega}_1}{4}\left(\frac{\lambda}{\bar{R}'_1} - \frac{\lambda}{\bar{R}'_2}\right) \cos \bar{\beta}_c = \frac{\omega_1}{4}\left(\frac{1}{R'_1} - \frac{1}{R'_2}\right) \cos(\beta_i - \beta_o) \quad , \\
&\bar{\omega}_2 \bar{R}_2 \cos(\bar{\beta}_t + \bar{\beta}_c) = \lambda\, \omega_2 R_2 \cos \beta_i \quad (\text{Note: } R_2 = R_p \sec \beta_i - R_1) \, , \\
&\bar{\omega}_2 \sin(\bar{\beta}_t + \bar{\beta}_c) = \omega_2 \sin \beta_i \quad , \\
&\frac{\bar{\omega}_2}{4}\left(\frac{\lambda}{\bar{R}'_1} - \frac{\lambda}{\bar{R}'_2}\right) \cos(\bar{\beta}_t + \bar{\beta}_c) = \frac{\omega_2}{4}\left(\frac{1}{R'_1} - \frac{1}{R'_2}\right) \cos \beta_i \quad .
\end{aligned}\right\} \text{I}$$

This is a system of eight equations determining eight parameters of the rolling-disk system, namely $\bar{R}_1$, $\bar{R}_2$, $\bar{R}'_1$, $\bar{R}'_2$, $\bar{\omega}_1$, $\bar{\omega}_2$, $\bar{\beta}_t$, and $\bar{\beta}_c$. Happily, the system can be solved analytically. Combining the third, fifth, sixth, and eighth equations properly shows that $\bar{R}_2/\bar{R}_1 = R_2/R_1$. It follows readily then that $\bar{R}_1 = \lambda R_1$ and $\bar{R}_2 = \lambda R_2$. Then the third and fourth equations imply that $\bar{\omega}_1 = \omega_1$, and the sixth and seventh imply that $\bar{\omega}_2 = \omega_2$. Then either the third and fifth or sixth and eighth equations imply

$$\frac{\lambda}{\bar{R}'_1} - \frac{\lambda}{\bar{R}'_2} = \frac{1}{R'_1} - \frac{1}{R'_2} \quad ,$$

and combining this with the second equation shows $\bar{R}'_1 = \lambda R'_1$ and $\bar{R}'_2 = \lambda R'$. Finally then, the third and fourth or sixth and seventh equations imply $\bar{\beta}_c = \beta_i - \beta_o$ and $\bar{\beta}_t + \bar{\beta}_c = \beta_i$.

What has been shown then is that the <u>only</u> selection of parameters permissible for the rolling-disk system to represent a given ball-race configuration is as follows:

$$\bar{R}_1 = \lambda R_1, \quad \bar{R}_2 = \lambda R_2, \quad \bar{R}'_1 = \lambda R'_1, \quad \bar{R}'_2 = \lambda R'_2,$$

$$\bar{\omega}_1 = \omega_1, \quad \bar{\omega}_2 = \omega_2, \quad \bar{\beta}_c = \beta_i - \beta_o, \quad \bar{\beta}_t = \beta_o \quad .$$

Of course, it is also necessary that $\bar{W} = \lambda^2 W$, and when one imposes the further condition that $\lambda = 1$, it can be seen that the only permissible combination of parameters in the rolling-disk system duplicates those of the ball-race system. If there is any difficulty associated with using those ball-race parameters (and there usually is!) then that difficulty is imposed on the rolling-disk experiment if this ideal level of simulation is to be achieved.

A Form of Close Simulation

A parameter of the ball-race system which would be particularly difficult to match in the rolling-disk machine is the angular velocity of the ball. In the bearing to be simulated that velocity is nearly 47,000 rpm. In order to reduce this velocity to a more reasonable level, some aspect of the simulation process must be compromised. The compromise to be chosen is somewhat arbitrary, but it seems reasonable to approach the choice by seeking to make the compromise as harmless as possible. To accomplish this, we may observe in Table 2 that $u_1 + u_2$ varies by only a few percent in either case considered there. Since changes of this magnitude should not affect either the lubricant film thickness or the pressure distribution[7,8] significantly in comparison to the expected accuracy of measurement of them, it seems reasonable to neglect consideration of the coefficients y and y^2 in $u_1 + u_2$ while choosing the disk parameters. The constant term of $u_1 + u_2$ can still be retained in the simulation, together with all three coefficients of $u_2 - u_1$. When this is done, System I is replaced by

$$\left.\begin{aligned}
&\frac{\lambda}{\bar{R}_1} + \frac{\lambda}{\bar{R}_2} = \frac{1}{R_1} + \frac{1}{R_2} \quad , \\
&\frac{\lambda}{\bar{R}'_1} + \frac{\lambda}{\bar{R}'_2} = \frac{1}{R'_1} + \frac{1}{R'_2} \quad , \\
&\bar{\omega}_1 \bar{R}_1 \cos \bar{\beta}_c = \lambda \omega_1 R_1 \cos (\beta_i - \beta_o) \quad , \\
&\bar{\omega}_2 \bar{R}_2 \cos (\bar{\beta}_t + \bar{\beta}_c) = \lambda \omega_2 R_2 \cos \beta_i \quad , \\
&\bar{\omega}_1 \sin \bar{\beta}_c + \bar{\omega}_2 \sin (\bar{\beta}_t + \bar{\beta}_c) = \omega_1 \sin (\beta_i - \beta_o) + \omega_2 \sin \beta_i \quad , \\
&\frac{1}{4} \left(\frac{\lambda}{\bar{R}'_1} - \frac{\lambda}{\bar{R}'_2}\right)[\bar{\omega}_1 \cos \bar{\beta}_c + \bar{\omega}_2 \cos(\bar{\beta}_t + \bar{\beta}_c)] = \frac{1}{4} \left(\frac{1}{R'_1} - \frac{1}{R'_2}\right)[\omega_1 \cos(\beta_i - \beta_o) + \omega_2 \cos \beta_i] .
\end{aligned}\right\} \text{II}$$

This is a system of six equations for the eight unknown parameters $\bar{R}_1$, $\bar{R}_2$, $\bar{R}'_1$, $\bar{R}'_2$, $\bar{\omega}_1$, $\bar{\omega}_2$, $\bar{\beta}_t$, and $\bar{\beta}_c$, so two of these parameters may be assigned arbitrarily. One obvious choice to make is $\bar{\omega}_2 = \bar{\omega}_1$, so that the burden of achieving the high

required angular velocities can be shared equally by the two disks. It would be nice to take also $\bar{R}_2' = \bar{R}_1'$, so that the disks could be crowned equally, but this choice would violate the last equation of System II. Thus, we choose instead to assign $\bar{\beta}_t = 0$, so that the axes of the disks can be kept parallel. Under the assumptions that

$$\bar{\omega}_2 = \bar{\omega}_1 \quad \text{and} \quad \bar{\beta}_t = 0 \quad ,$$

the System II can be solved by a process much like that applied to System I. If we use the notation

$$u_{10} = R_1\omega_1\cos(\beta_i-\beta_o),\ u_{11} = -\omega_1\sin(\beta_i-\beta_o),\ u_{12} = -\frac{\omega_1}{4}\left(\frac{1}{R_1'}-\frac{1}{R_2'}\right)\cos(\beta_i-\beta_o),$$

$$u_{20} = R_2\omega_2\cos\beta_i,\ u_{21} = \omega_2\sin\beta_i,\ u_{22} = \frac{\omega_2}{4}\left(\frac{1}{R_1'}-\frac{1}{R_2'}\right)\cos\beta_i \ ,$$

these being simply the three coefficients of $u_1(y)$ and of $u_2(y)$ respectively, then the solution of System II can be written as

$$\bar{R}_1 = \lambda R\left(1+\frac{u_{10}}{u_{20}}\right) \qquad \bar{R}_2 = \lambda R\left(1+\frac{u_{20}}{u_{10}}\right) \quad ,$$

$$\bar{R}_1' = \lambda\Big/\left[\frac{1}{2R'} + R(u_{22}-u_{12})\left(\frac{1}{u_{10}}+\frac{1}{u_{20}}\right)\right] \quad ,$$

$$\bar{R}_2' = \lambda\Big/\left[\frac{1}{2R'} - R(u_{22}-u_{12})\left(\frac{1}{u_{10}}+\frac{1}{u_{20}}\right)\right]$$

$$\bar{\omega}_1 = \left[\frac{u_{10}^2u_{20}^2}{R^2(u_{10}+u_{20})^2} + \frac{(u_{21}-u_{11})^2}{4}\right]^{1/2} \qquad (=\bar{\omega}_2) \quad ,$$

$$\tan\bar{\beta}_c = \frac{R(u_{21}-u_{11})(u_{10}+u_{20})}{2\,u_{10}u_{20}} \quad , \qquad (\text{and } \bar{\beta}_t = 0) \quad .$$

To resolve any doubt about whether the arbitrary assignment of the parameters $\bar{\omega}_2$ and $\bar{\beta}_t$ creates unacceptable changes in the $\bar{y}$ and $\bar{y}^2$ terms of $\bar{u}_1+\bar{u}_2$, it may be observed readily from the equations for $\bar{u}_1(\bar{y})$ and $\bar{u}_2(\bar{y})$ that taking $\bar{\omega}_2 = \bar{\omega}_1$ and $\bar{\beta}_t = 0$ simply makes those two terms of $\bar{u}_1(\bar{y}) + \bar{u}_2(\bar{y})$ vanish, and conversely that making those terms vanish implies that $\bar{\omega}_1 = \bar{\omega}_2$ and $\bar{\beta}_t = 0$. Since

these terms were supposed to be small compared to the constant term, this approximation should be quite acceptable.

For the two cases of ball-race contact described by Tables 1 and 2, the disk parameters needed for this approximate simulation are as follows:

Parameter	Value for Case 1	Value for Case 2
$\bar{R}_1$, in.	0.71834λ	0.71878λ
$\bar{R}_2$, in.	0.71364λ	0.71431λ
$\bar{R}'_1$, in.	0.40527λ	0.40531λ
$\bar{R}'_2$, in.	-0.43761λ	-0.43765λ
$\bar{\omega}_1 (= \bar{\omega}_2)$, rpm	26707	26624
$\bar{\beta}_c$, deg	10.828	9.679
$\bar{\beta}_t$, deg	0.000	0.000
$\bar{W}$, lb	$489.04\lambda^2$	$841.04\lambda^2$

Of course, for complete thermal similitude, one also should have $\lambda = 1$.

Possible objections to these parameters for experimental use are that $\bar{R}_1$ and $\bar{R}_2$ are small and that $\bar{R}'_2$ is negative (so that one disk has an inverted crown). The smallness of $\bar{R}_1$ and $\bar{R}_2$, however, probably is beneficial for our present rolling-disk equipment which is somewhat limited in the loads it can tolerate. In order to avoid the negative $\bar{R}'_2$, some further compromise of the similarity must be made.

A Convenient Form of Simulation

In order to avoid negative curvature on both disks, some further aspect of similarity must be neglected. The choice here is not so painless as in the previous approximation, but one more fairly reasonable approximation is available. It is to disregard similarity as it affects the constant and the quadratic terms of u_2-u_1. Keeping the linear term provides variable slip between the surfaces, and the discrepancy between that slip and the slip of the two cases of

ball-race contact under consideration reaches only about 30 percent of the maximum calculated slip. If we keep also the constant term of $u_1 + u_2$ in arranging similarity, but again drop the linear and quadratic terms, the Systems I and II are now replaced by the following system:

$$\left.\begin{aligned}
&\frac{\lambda}{\bar{R}_1} + \frac{\lambda}{\bar{R}_2} = \frac{1}{R_1} + \frac{1}{R_2} \quad , \\
&\frac{\lambda}{\bar{R}'_1} + \frac{\lambda}{\bar{R}'_2} = \frac{1}{R'_1} + \frac{1}{R'_2} \quad , \\
&\bar{\omega}_1 \bar{R}_1 \cos\bar{\beta}_c + \bar{\omega}_2 \bar{R}_2 \cos(\bar{\beta}_t + \bar{\beta}_c) = \lambda\omega_1 R_1 \cos(\beta_i - \beta_o) + \lambda\omega_2 R_2 \cos\beta_i \quad , \\
&\bar{\omega}_1 \sin\bar{\beta}_c + \bar{\omega}_2 \sin(\bar{\beta}_t + \bar{\beta}_c) = \omega_1 \sin(\beta_i - \beta_o) + \omega_2 \sin\beta_i \quad .
\end{aligned}\right\} \quad \text{III}$$

Now there are only four equations relating the eight unknowns $\bar{R}_1$, $\bar{R}_2$, $\bar{R}'_1$, $\bar{R}'_2$, $\bar{\omega}_1$, $\bar{\omega}_2$, $\bar{\beta}_t$, and $\bar{\beta}_c$, so four of those unknowns may have values assigned to them arbitrarily. Two obvious choices to make are $\bar{\omega}_2 = \bar{\omega}_1$ and $\bar{\beta}_t = 0$, so these will be taken. Another obvious choice, which is now acceptable since the quadratic terms of both $u_1 + u_2$ and $u_2 - u_1$ are being ignored, is that $\bar{R}'_2 = \bar{R}'_1$. To this we add the choice that $\bar{R}_2 = \bar{R}_1$, since this will make the two disks geometrically alike, and that likeness will make the lubricant film as flat as possible and facilitate possible passage of X-rays for film-thickness measurements. With these assigned values, the solution of System III becomes

$$\bar{R}_1 = \bar{R}_2 = 2\lambda R \quad , \quad \bar{R}'_1 = \bar{R}'_2 = 2\lambda R'$$

$$\bar{\omega}_1 = \left[\frac{1}{16R^2}(u_{10} + u_{20})^2 + \frac{1}{4}(u_{21} - u_{11})^2\right]^{1/2} \quad (= \bar{\omega}_2)$$

$$\tan\bar{\beta}_c = \frac{2R(u_{21} - u_{11})}{u_{10} + u_{20}} \quad , \quad (\text{and } \bar{\beta}_t = 0) \quad .$$

The effect of the assignments $\bar{\omega}_2 = \bar{\omega}_1$, $\bar{\beta}_t = 0$, $\bar{R}_1 = \bar{R}_2$, and $\bar{R}'_1 = \bar{R}'_2$ on $\bar{u}_1(\bar{y}) + \bar{u}_2(\bar{y})$ and $\bar{u}_2(\bar{y}) - \bar{u}_1(\bar{y})$ is simply to make the linear and quadratic terms of the sum vanish, and to make the constant and quadratic terms of the difference vanish. These are approximations which should be widely acceptable, though this approximation in $\bar{u}_2(\bar{y}) - \bar{u}_1(\bar{y})$ is somewhat poorer than the previous approximation.

For this last approximate simulation, the parameters needed for the disks corresponding to the ball and race for the cases described by Tables 1 and 2 are as follows:

Parameter	Value for Case I	Value for Case II
$\bar{R}_1$, in.	0.71598λ	0.7165λ
$\bar{R}_2$, in.	0.71589λ	0.7165λ
$\bar{R}_1'$, in.	10.9688λ	10.9688λ
$\bar{R}_2'$, in.	10.9688λ	10.9688λ
$\bar{\omega}_1 (= \bar{\omega}_2)$, rpm	26707	26721
$\bar{\beta}_c$, deg	10.828	9.679
$\bar{\beta}_t$, deg	0.000	0.000
W, lb	$489.04\lambda^2$	$841.04\lambda^2$

Complete thermal similitude again demands that $\lambda = 1$.

The Effect of Further Compromise of Similarity

The set of parameters suggested in the last preceding list should provide reasonably good similarity between rolling-disk experiments and the ball-race system, and they should also be relatively usable experimentally. Problems that may yet occur with simulations of this sort are that the disks may need to have slightly larger radii, and it may not be possible to drive the disks entirely up to the specified speeds. These difficulties will be overcome by refining the experimental arrangements if this is feasible, but if this refinement cannot be made entirely, we can still estimate the effect of such deficiencies by reviewing the simulation theory which has been provided.

If it is necessary to take the relative rolling radius greater for the disks than for the ball bearing, that is $\bar{R} > R$ or $\lambda > 1$, then both the rolling

and crown radii of both disks should be increased by the same factor λ, and the applied load should be increased by the factor λ^2. The effect of such an expansion will be to increase the local thermal disturbances, since the thermal conductivity of the lubricant and bearing material will not have been increased by the factor λ^2 as similarity principles would require. Thus, if one took $\lambda = 2$, the magnitude of the temperature variations would be roughly quadrupled, and effects dependent on the lubricant viscosity would be magnified accordingly. One way to gage such effects experimentally would be to perform two experiments using different values of λ, but this is perhaps too expensive a technique to use for the present. It seems better just to make λ as close to unity as possible, and to estimate the thermal effects as has been indicated.

If it proves impossible to run the experiments at the desired rates of revolution, then a sequence of experiments can be run at several different lower rates, and an estimate of values to be expected at the full rate can be made by extrapolation. Of course, it will be desirable to make the extrapolation as short as possible, that is to have one experiment approach the desired speed as closely as possible. Problems with speed have been experienced through power limitations of the motors, and vibrations eventually might arise. Our experiments to date have used fairly light slip between the disks, and the slip processes may prove quite power consuming. If difficulties with power are very bad, it would be possible, of course, to reduce $\bar{\beta}_c$, the angle of inclination of the contact area, but this would represent another deficiency of simulation with effects that could be corrected probably only by extrapolation of the experimental results.

OBSERVATIONS TO BE MADE EXPERIMENTALLY

Conditions have been determined to make rolling-disk experiments simulate lubrication in the ball bearing of interest to the NASA Lewis Research Center

to various degrees of accuracy. However, some other matters relevant to experiments also deserve consideration. Thus the experimental program to be chosen should account for both these kinds of consideration.

The distinctive features of the planned experiments are that they are to be closely related to the operation of a particular bearing, and that they are to include, in particular, some simulation of the nonuniform sliding between the bearing surfaces. The simulation of nonuniform sliding represents a new experimental condition, and as such should be treated so that its principal effects can be identified, though it should not be necessary to simulate all details of the sliding in the early stages of experimentation. Since the sliding is expected to be most influential by way of its thermal effects, it is very desirable to seek good simulation of the temperature distribution. To achieve this, the geometric expansion factor λ applied to the relative rolling radius should be as near to unity as possible. Thus it is intended to take $\lambda = 1$.

The high rolling speeds required for ideal simulation of the ball bearing appear prohibitive, so one of the approximate forms of simulation is much to be preferred. Beyond this, since X-ray measurements of film thickness are to be made, it becomes quite desirable for both disks to have the same rolling radii and the same crown radii. The choice of this symmetry entails some loss in the simulation of sliding between the surfaces, but that loss is not large enough to deny the virtue of choosing symmetric disks. Therefore, the method of simulation described above as "convenient" will be used. This method produces surface sliding that varies linearly from side to side of the contact area and vanishes at the center. (Close simulation of the sliding at both ends of the disks still may be achieved by driving one disk a little faster and the other disk the same amount slower, though such differential driving worsens the simulation of the slip rate at the center of contact.) The disks to be used will have diameters

of approximately 1.41 in. (= 2 x 0.717 cos 9.68°) to their centers of contact, and their crown radii will be about 11.0 in.

It is inconvenient to require many sets of disks, especially for no greater persuasion than to make the cone angle $\bar{\beta}_c$ vary slightly as the load is changed. Therefore, the same cone angle will be used regardless of the load, and that angle will be taken to be about 10 degrees. This will tend to make the sliding slightly less or more than the desired value according as the maximum Hertz pressure is less or more than about 310,000 psi. However, while no variation of $\bar{\beta}_c$ according to load is planned, it is believed that control experiments are very desirable to gage the actual influence of sliding on the lubrication processes. Therefore, it is planned to perform a complementary set of experiments using disks without coned surfaces, that is with $\bar{\beta}_c = 0$.

The rolling speed of the surface of a disk with disk-radius 1.41 in. rotating at 26721 rpm is 1976 in./sec or 9882 ft.min. This speed is the one required for simulation of Case II operation of the prototype ball bearing according to the "convenient" simulation procedure. Of course, experiments should be performed at varying speeds, so it is suggested here that a good set of experimental rolling velocities would be 2,000, 4,000, 6,000, 8,000, and 10,000 ft/min for each disk. If vibrations or power limitations preclude achievement of the highest velocity, then experiments should be performed at velocities as high as possible.

The maximum Hertz pressures in Cases I and II as stated for the ball bearing are approximately 269,000 and 322,000 psi. There is also some interest in what may happen if this pressure goes as high as 400,000 psi. Of course, a frequently used level in the earlier Battelle studies was 100,000 psi. Thus it seems that a reasonable set of maximum Hertz pressures to be used in selecting

experimental conditions for the present program is 100,000, 175,000, 250,000, 325,000, and 400,000 psi. Loads which should produce these are easily computed, since maximum Hertz pressure varies as the cube root of the load, and the pressure 322,000 psi is produced by a normal load of 841 lb on the disks that are here proposed. (Note that getting an 841-lb normal load requires a diametral load of 841 cos 10° = 828 lb and a thrust load of 841 sin 10° = 146 lb.)

The film thicknesses are being measured by counting X-rays transmitted through the lubricant film in the contact area. The X-rays are projected in the direction of rolling, and since there is some reason to expect the films to be thinner near the ends than near the center[9], measurements of film thickness will be made at many axial positions.

At positions away from the center line, the disk radii will be unequal, and this will warp the lubricant film and cause some loss of X-ray transmission. The warpage should be the same as that of the surface midway between the disks before they are deformed. At distance $\bar{x}$ in the rolling direction and $\bar{y}$ in the axial direction from the center of contact, the deflection of that midway surface from the central tangent plane is (Cf. Figure 2):

$$\delta(\bar{x},\bar{y}) = \frac{\bar{x}^2}{4}\left[\frac{1}{\bar{r}_2 \sec(\bar{\beta}_c - \frac{\bar{y}}{\bar{R}_2'})} - \frac{1}{\bar{r}_1 \sec(\bar{\beta}_c + \frac{\bar{y}}{\bar{R}_1'})}\right] + \frac{\bar{y}^2}{4}\left[\frac{1}{\bar{R}_2'} - \frac{1}{\bar{R}_1'}\right] ,$$

where $\bar{r}_1 = \bar{r}_{1c} - \bar{y} \sin \bar{\beta}_c - \frac{\bar{y}^2}{2\bar{R}_1'} \cos \bar{\beta}_c$ and $\bar{r}_2 = \bar{r}_{2c} + \bar{y} \sin \bar{\beta}_c - \frac{\bar{y}^2}{2\bar{R}_2'} \cos \bar{\beta}_c$.

Then if $\bar{R}_1 = \bar{R}_2$, $\bar{R}'_1 = \bar{R}'_2$, so that $\bar{r}_{1c} = \bar{r}_{2c}$ (these being center-of-contact disk radii),

$$\delta(x,y) = -\frac{\bar{x}^2\bar{y}\,\sin\bar{\beta}_c\,\cos\bar{\beta}_c}{2\,\bar{r}_{1c}^2} \cdot \frac{\cos\dfrac{\bar{y}}{\bar{R}'_1} - \dfrac{\bar{R}_1}{\bar{y}}\sin\dfrac{\bar{y}}{\bar{R}'_1} + \dfrac{\bar{y}}{2\bar{R}'_1}\sin\dfrac{\bar{y}}{\bar{R}'_1}}{1 - \left[\tan^2\bar{\beta}_c + \dfrac{\bar{R}_1}{\bar{R}'_1}\right]\dfrac{\bar{y}^2}{\bar{R}_1^2} + \dfrac{\bar{y}^4}{4\bar{R}_1^2\bar{R}_1'^2}}$$

$$\approx -\frac{\bar{x}^2\bar{y}\,\sin\bar{\beta}_c\,\cos\bar{\beta}_c}{2\,\bar{r}_{1c}^2}\left[1 - \frac{\bar{R}_1}{\bar{R}'_1}\right] .$$

The greatest value of this deflection in the dry-contact area occurs on the boundary ellipse at $\bar{y} = \bar{y}_h / \sqrt{3}$ and is

$$\delta_{max} \approx -\frac{\sqrt{3}\,\bar{x}_h^2\bar{y}_h\,\sin\bar{\beta}_c\,\cos\bar{\beta}_c}{9\,\bar{r}_{1c}^2}\left[1 - \frac{\bar{R}_1}{\bar{R}'_1}\right] .$$

Taking representative values $\bar{x}_h = 0.01456$ in., $\bar{y}_h = 0.0855$ in., $\bar{r}_{1c} = 0.706$ in. (= 0.717 cos 10°, inch), and $\bar{\beta}_c = 10°$ makes this $\delta_{max} = -1.12 \times 10^{-6}$ in. This distance is small enough so that the warpage of the lubricant film should not cause any great loss in X-ray transmission, and it should be possible to correct for such a loss if that is necessary.

Consideration had been given to measuring film-thickness profiles using X-rays projected across the contact area in the axial direction (circumferential profile), but it is now recommended that such measurements should be deferred.

There is a strong possibility that the rolling surfaces dip toward each other along a curve approximating the trailing edge of contact.[9] In such a case, the film thickness would vary in a pattern hard to detect by X-rays projected in the axial direction, and measurements using those X-rays would add little to the information obtainable from X-rays projected in the rolling direction (axial profile). Since also the rolling-disk machine lacks adequate space for axial projection of X-rays when the disks are as small as now seem needed, the use of such projection apparently should be deferred.

Both pressure distributions and lubricant film thicknesses are potentially important factors affecting bearing life. Therefore, measurements of pressure as well as film thickness might be desirable. If pressure were measured, it would be by using manganin pressure transducers shaped so as to measure spot pressures (that is, pressures over regions with both length and width small with respect to the length and width of the contact area). Difficult with such measurements would be expected at higher temperatures, since transducers have not yet been used for $T > 350$ F.

Various lubricants will be used, of course, these being ones that are NASA candidate oils for the ball bearing under consideration. The operating temperatures for them should represent levels expected by NASA when possible.

Thus, the recommended design parameters and measurements to be used experimentally are those shown in Table 3. It is <u>not</u> suggested that all combinations of these parameters should be used; it is suggested merely that the parameters for any experiment should be drawn from values suggested in the table. The geometry recommended is shown in Figure 3.

TABLE 3. SPECIFICATIONS SUGGESTED FOR ROLLING-DISK EXPERIMENTS

Parameter or Measurement	Suggested Choices
Disk radii ($\bar{R}_1 \cos \bar{\beta}_c = \bar{R}_2 \cos \bar{\beta}_c$)	0.71 in.
Crown radii ($\bar{R}'_1 = \bar{R}'_2$)	11.0 in.
Cone angle ($\bar{\beta}_c$)	0°, 10°
Axial tilt angle ($\bar{\beta}_t$)	0°
Rolling speed ($\bar{r}_{1c}\bar{\omega}_1 = \bar{r}_{2c}\bar{\omega}_2$)	2,000 (2,000) 10,000 ft/min
Maximum Hertz pressure (p_h)	100,000 (75,000) 400,000 psi
Lubricants	NASA candidate lubricants
Temperatures	250 F to 600 F
Pressure measurement	Manganin transducer for T < 350 F
Film-thickness measurement	X-rays in rolling direction

The required load varies as p_h^3. For p_h measured in $lb/in.^2$, the proportionality factor would be 25078×10^{-18} for Case 1, or 25105×10^{-18} for Case 2. Thus a good value in any case is

$$W = 25100\ (10^{-6}\ p_h)^3 \text{ for } p_h \sim lb/in.^2.$$

This normal load should be multiplied by cos10° to find the diametral load (that is, the directly applied load).

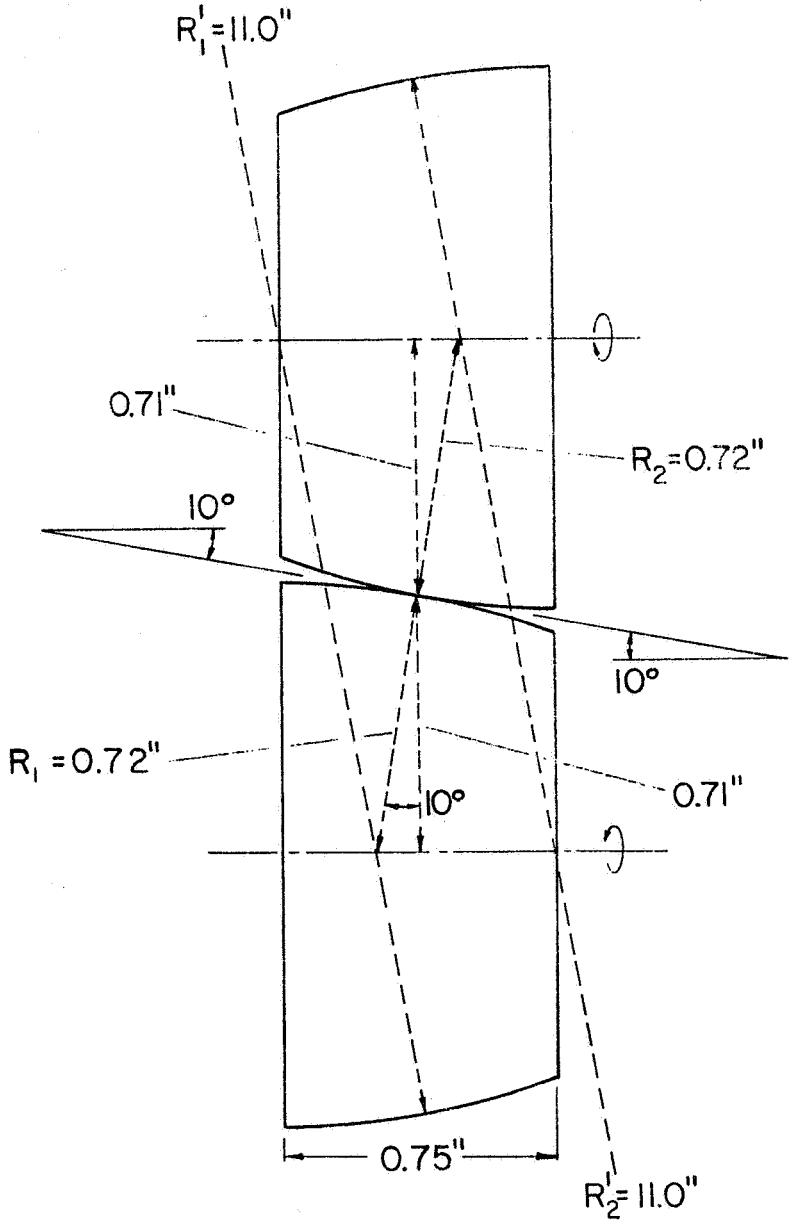

FIGURE 3. RECOMMENDED GEOMETRY FOR CONED DISKS

EXPERIMENTAL STUDIES WITH SIMILITUDE DISKS

By means of the similitude analysis it was possible to define accurately a disk geometry to be used in the lubrication experiments. This geometry is summarized in Table 3. The next step in the research program then was to evaluate the feasibility of conducting disk lubrication experiments with this geometry under severe operating condition of loads, speeds, and temperatures. The targets for these conditions were simulation of loads to 400,000 psi maximum contact pressures, full bearing speeds to 12500 rpm and temperatures to 600 F.

Description of Basic Apparatus

The rolling-disk apparatus which was developed for use in this study is shown pictorially in Figure 4. Each of the contacting disks is driven by a 5 HP variable-speed high-frequency induction motor; disk and motor rotor are both mounted on the same shaft. These shafts are supported by precision (ABEC-7) duplex ball bearings; the main support bearings, adjacent to the disks, are 45-mm bore, and the outboard bearings are 35-mm bore. The bearings are lubricated and cooled by a jet lubrication system. Disk loading is accomplished through a cantilever beam actuated by a pneumatic cylinder.

Various adjustments allow the disks to be positioned quite accurately with respect to each other. The lower disk assembly may be positioned axially with respect to the upper through a dovetail mounting. The lower assembly may also be swiveled in a horizontal plane to eliminate skewing at the contact area. Finally, the axis of the upper disk assembly may be tilt-aligned with that of the lower by means of jackscrews built into the base plate.

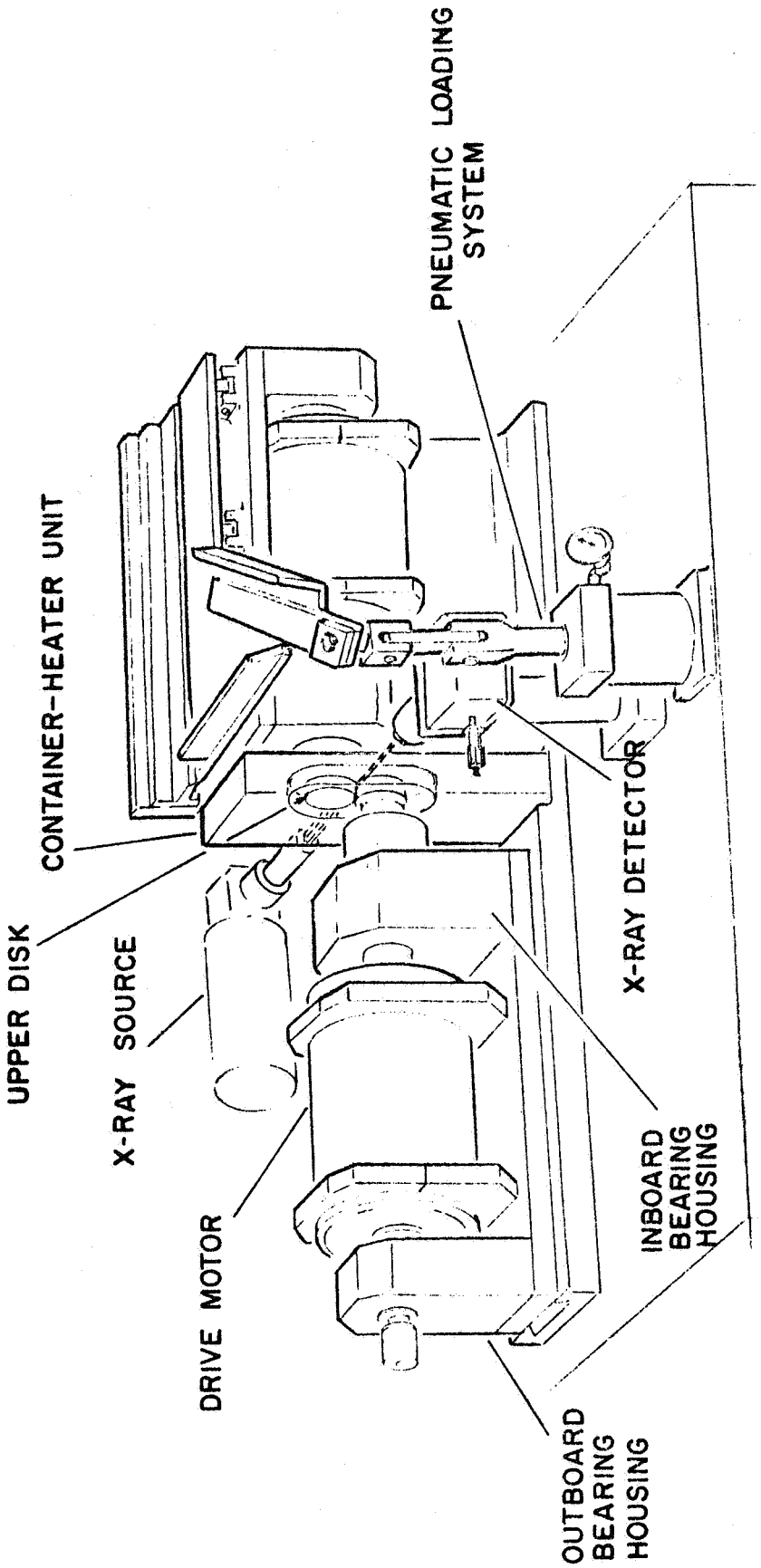

FIGURE 4. PICTORIAL DRAWING OF DISK APPARATUS USED IN LUBRICATION EXPERIMENT

A recirculating lubrication system is used for the disks, with the supply pump submerged in the oil pump. Lubricant is fed to the contact zone by means of an oil jet, and is scavenged by a gravity return to the sump. The lubricant is filtered and preheated before entering the contact zone. The disks are enclosed in a special "can" arrangement which serves as a container for the lubricant and contains the heaters for the disk. The can region is designed to operate above 600 F, which is significantly higher than the temperature limit of the support bearings. Heat must be continuously supplied to the disks and removed from the bearings to maintain this required temperature differential.

Instrumentation

Perhaps the most critical aspect of the lubrication process occurring between rolling-contact disks is the thickness of the elastohydrodynamic lubricant film which is formed. The primary instrumentation to be used with the disk rig, then, is an X-ray technique for measuring this film thickness. As a supplement to this technique, dielectric-strength measurements are being used to observe the extent of fluid film breakdown.

The Battelle X-ray technique was described by Sibley and Austin[1]. It consists essentially of flooding the contact region between the disks with X-rays and of measuring the rate of transmission of X-rays by the lubricant film. The X-rays are absorbed only slightly by the lubricant but find the steel quite opaque. Thus, the rate of X-ray transmission can be related, by an appropriate calibration factor, to the film thickness.

Figure 5 is a schematic diagram of the X-ray system. An X-ray source tube is used which emits X-rays in a vertical "line" pattern. A metal shield

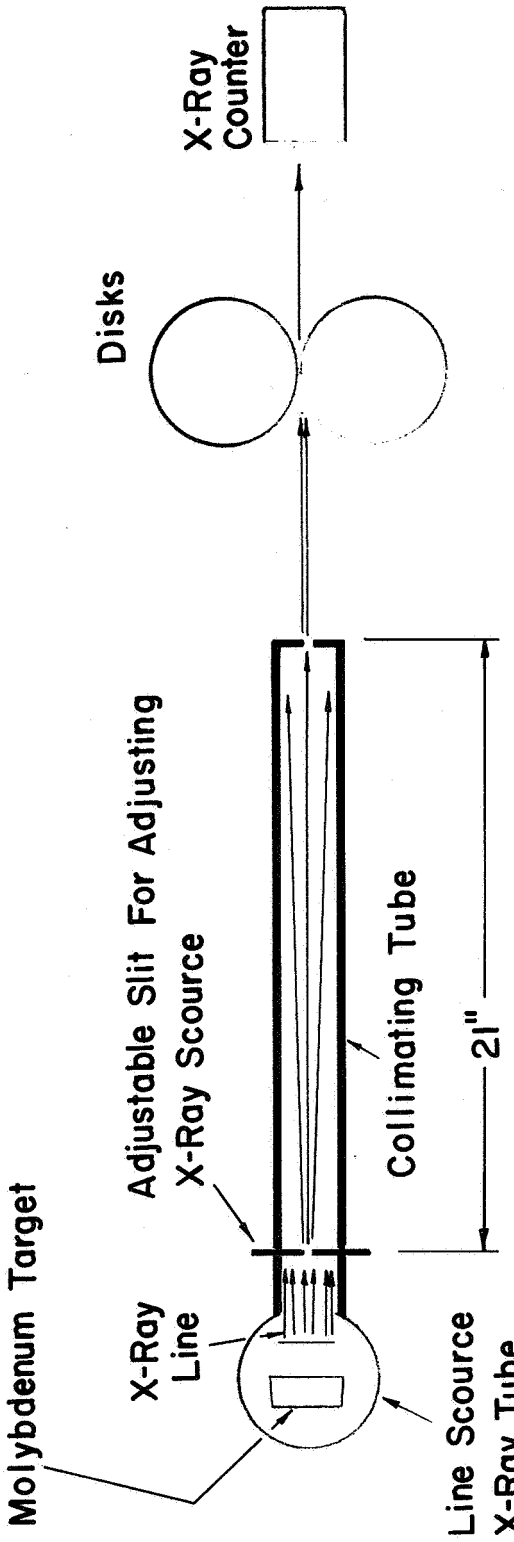

FIGURE 5. SCHEMATIC DRAWING OF X-RAY FILM THICKNESS MEASURING SYSTEM

containing a horizontal slit about 0.01 in. high is located in front of this line source. By moving the slit vertically, the elevation of the X-ray beam is controlled. The beam then diverges into a collimating tube. At the end of this tube is a slit about 1/8-in. high, oriented parallel to the plane of the disk contact area. The resulting line pattern through the slit is parallel and uniform.

The beam now passes through the contact zone between the disks and is detected at the other end by a scintillation counter, in front of which is fixed a third slit, oriented perpendicular to the plane of the contact region. The counter is transversed across the contact region in predetermined increments, giving a measure of the beam intensity, or count, at each increment. In this manner, a profile of the film thickness across the entire width of the disk can be found.

Calibration of the X-ray technique is obtained by spreading the disks in small amounts by means of a precise adjusting screw, and meanwhile observing the X-ray count for these known separations. A typical calibration curve is given in Figure 6; the lubricant in use was XRM-177.

In addition to the X-ray instrumentation, provision for observing the dielectric strength of the lubricant film has been incorporated into the apparatus. A schematic diagram of this circuit is given in Figure 7. One disk is electrically isolated from the other; an a-c voltage is applied across the disks and the extent of film breakdown is monitored by means of an oscilloscope.

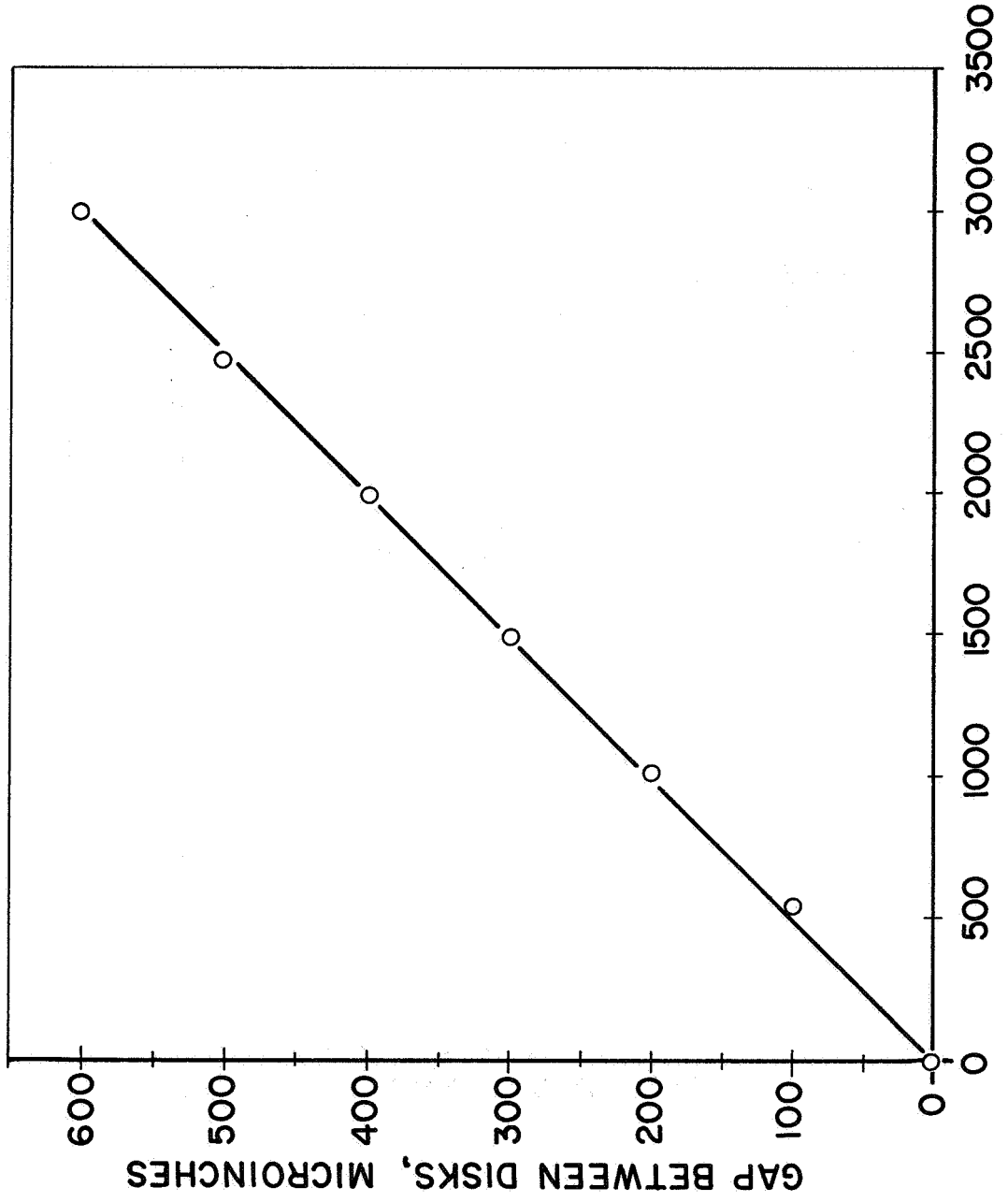

FIGURE 6. CALIBRATION OF X-RAY SYSTEM

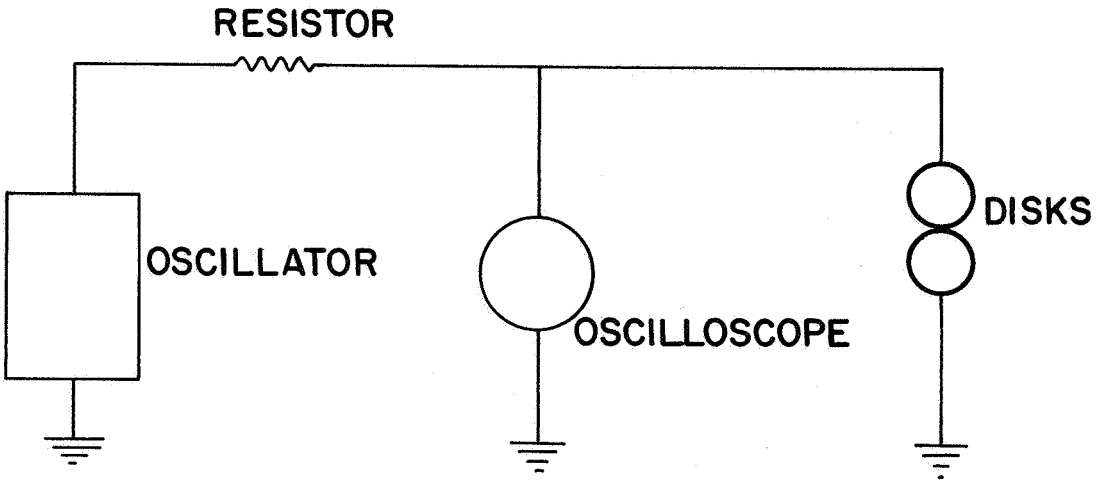

FIGURE 7. SCHEMATIC DIAGRAM OF LUBRICANT-FILM DIELECTRIC-STRENGTH MEASUREMENT CIRCUIT

Modification of Apparatus for High-Load, High-Temperature Studies

The disk apparatus was originally designed for performing experiments with six-inch-diameter disks at temperatures around 400 F. The high-temperature conditions to be encompassed by the program, and the disk specifications of Table 3, necessitated some modifications to the original apparatus. One of the primary objectives of Task II, therefore, was to make and test the required modifications. This primarily involved the utilization of much smaller disks, and the minimization of possible problems of corrosion and contamination associated with the operation, for sustained periods of time, at lubricant temperatures up to 600-700 F.

Features Incorporated into Apparatus to Allow for High-Temperature Experiments

The disks are operated in a nitrogen environment to prevent oxidation of the lubricant being evaluated. Nitrogen is also forced into the center of the labyrinth seal between each disk and the adjacent support bearing, to minimize any back flow of air into the inerted disk chamber. Flow meters have been provided to monitor nitrogen flow to each of these areas.

The disk chamber is totally enclosed by a second chamber. Sheath heaters for heating the disk to the desired operating temperature are brazed to the outside surface of this enclosure. A cutaway view of the disk container/heater is given in Figure 8. Figure 9 is an exterior view of the container with the upper disk removed. One problem in heating the disks is that the surrounding environment must be significantly cooler than the disk surface. The support bearings should not be heated in excess of 350 F, and some of the X-ray components such as the counter tube must be essentially at room temperature. The double-can arrangement has worked remarkably well in controlling and containing the heated region.

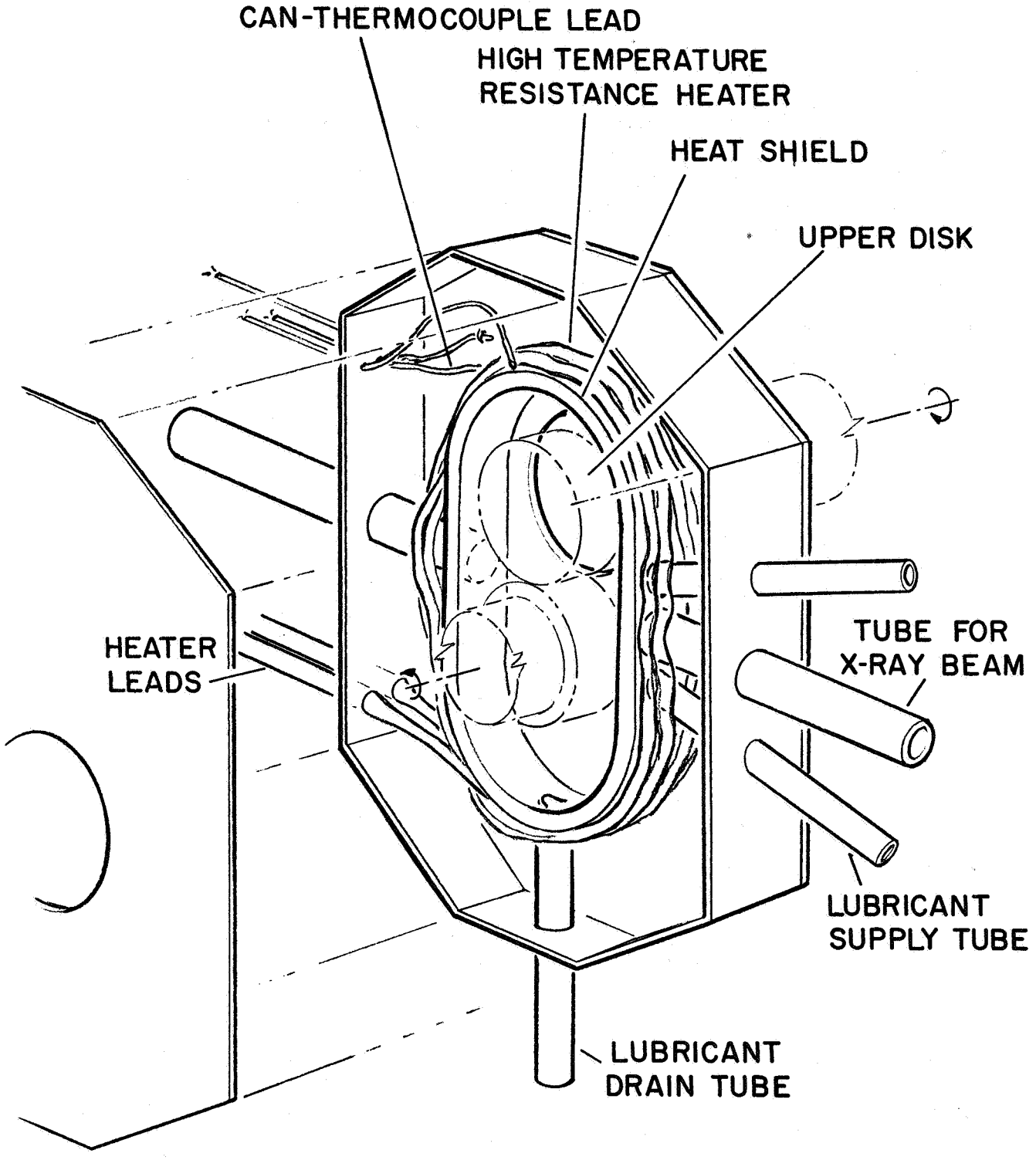

FIGURE 8. CUTAWAY VIEW OF DISK CONTAINER/HEATER

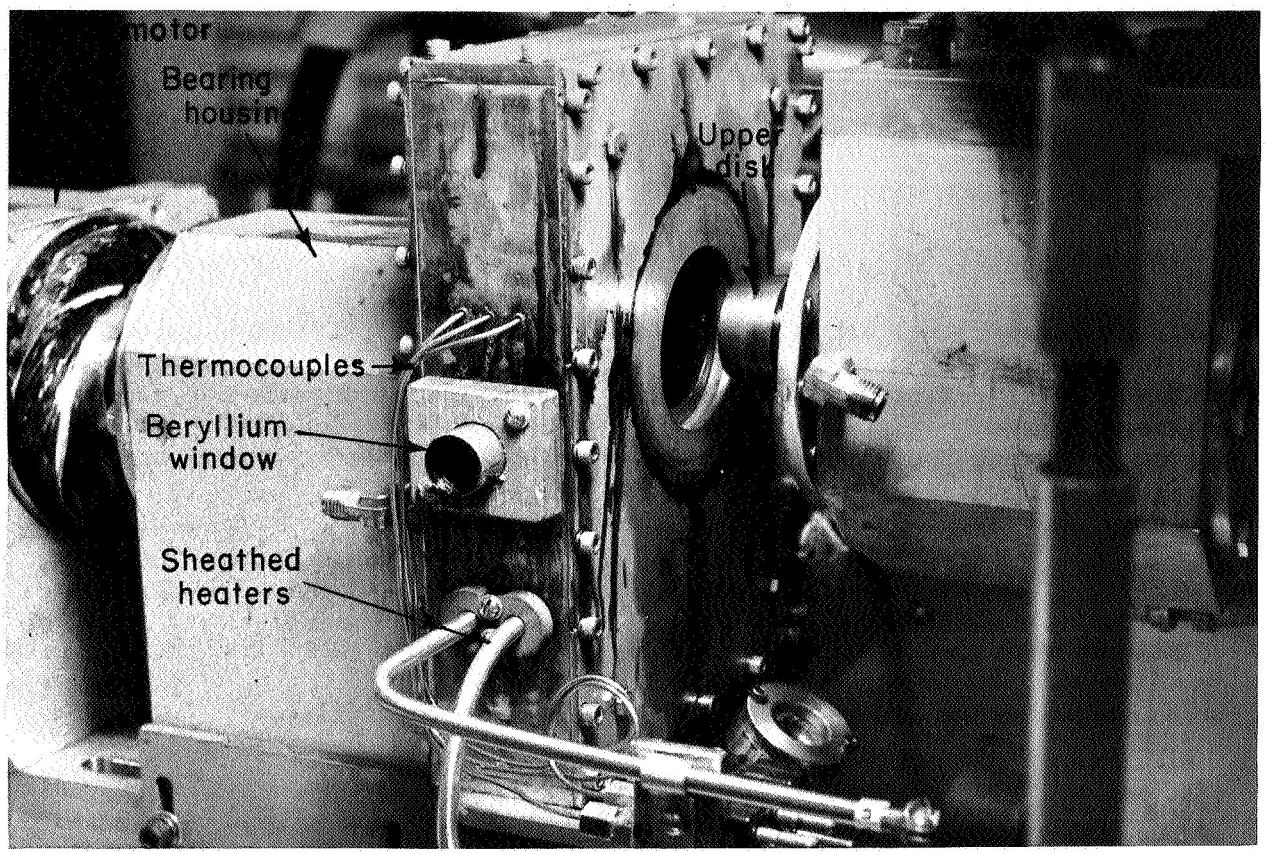

FIGURE 9. EXTERIOR VIEW OF DISK CONTAINER/HEATER WITH CONTAINER PULLED AWAY FROM UPPER DISK

Lubricant is supplied to the disks through a jet located at the inlet zone of the contact region. The lubricant is pumped through two heat exchangers upstream of the contact zone to preheat the lubricant to the desired temperature. In addition, high-capacity heat tapes surrounding the disk-lubricant plumbing lines and sump aid in maintaining the bulk of the lubricant at a preset temperature. Chromel-alumel thermocouples are used to measure temperatures at the disk surface, the lubricant inlet manifold, two points on the disk chamber, the lubricant sump, and both outboard bearings. These temperatures are read out on a multipoint recorder.

A schematic diagram of the lubrication system is given in Figure 10. The disk-lubricant lines including all component tubing, fittings, valves, and gages are made of stainless steel. To avoid temperature degradation of the disk-lubricant-pump main-shaft seal and consequent contamination of the lubricating fluid, this seal has been eliminated altogether. This was made possible by designing an enclosure (also nitrogen-pressurized) for the entire pump, such that the pump operates completely immersed in lubricant. This enclosure is also utilized as a sump for the bulk of the lubricant in the system.

Fabrication of Similitude Disks

As a result of the analyses, it was concluded that simulation of the ball-race lubrication of the 120-mm-bore angular-contact ball bearing could be obtained with a pair of rolling-disks by proper selection of the disk geometry. It was also tactily concluded that the use of disks of other than the proper geometry would yield, at best, results that would be questionable when related to that bearing. The disks must be very small, 1.42 in. in diameter, and have a cone angle of 10 degrees and a crown radius of 11 in. (see Table 2). Such disks, although basically feasible, were significantly different from those

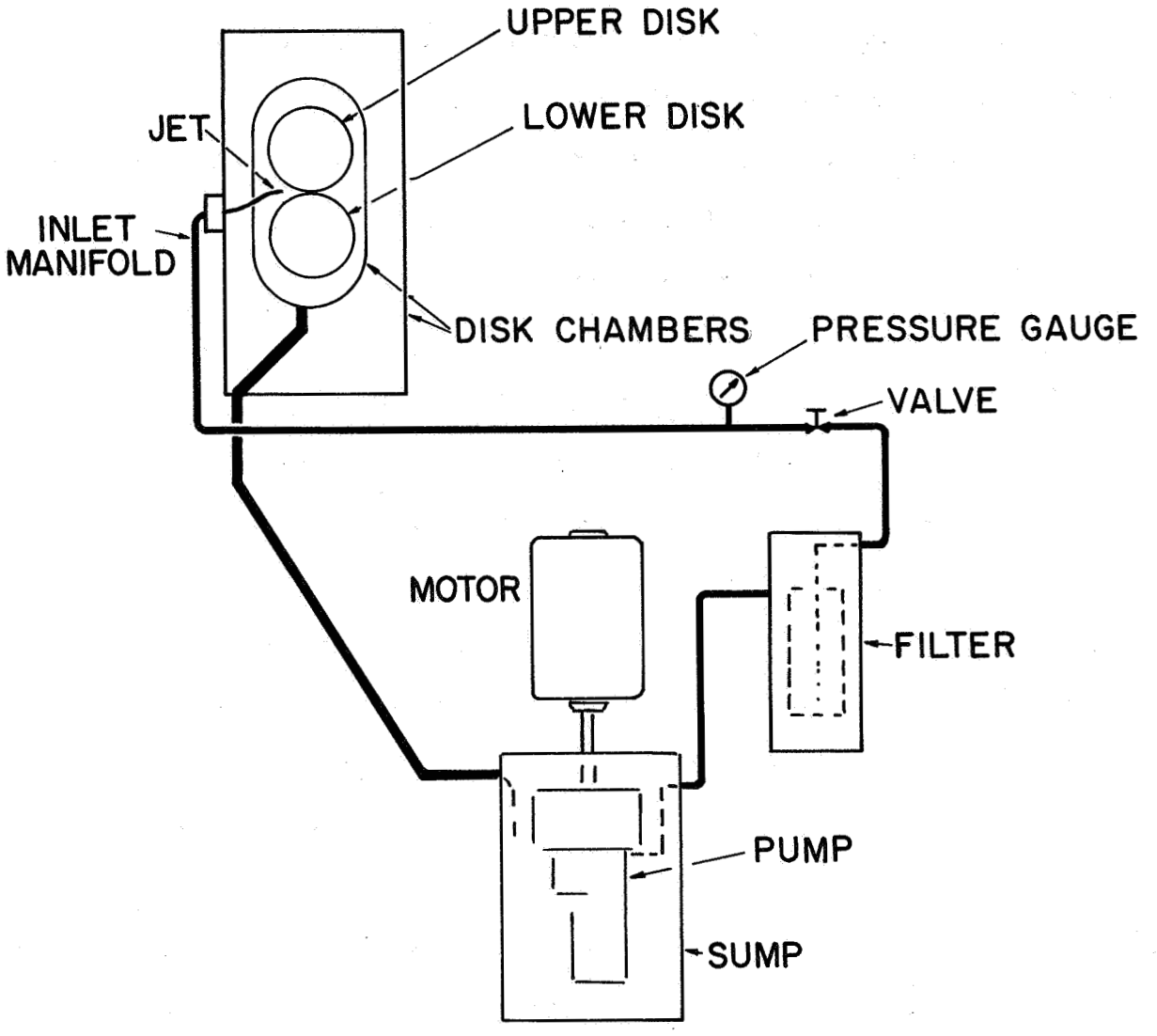

FIGURE 10. DISK LUBRICATION SYSTEM

that the experimental apparatus had been designed to accommodate. However, in order to evaluate accurately the feasibility of using the disk apparatus for lubrication experiments it was mandatory that this apparatus be evaluated under conditions which properly simulated the actual operating conditions. Actually, two types of disks are needed for the study. One type is the coned disk described above; the second is similar, but without the 10 degree cone angle.

The fabrication of 1.42-in.-diameter disks presented a few unique problems in the program since these disks were smaller in diameter than the supporting shaft at the main support (45-mm) bearings. Special shafts were, therefore, needed to accommodate the disks. The shaft design chosen involved a permanent attachment of the disks to the shaft. The shafts were fabricated from tool steel, through-hardened to R_c45. For proper simulation, the disks were made from high-temperature M50 bearing steel hardened to R_c60. The heat treatment for the disks was consistent with the required procedure for M50. A photograph of the disk/driving shaft arrangement is shown in Figure 11. Integral with each disk is a small stub-shaft which is pressed into the shaft with a 0.003 in. interference fit. Since the disk will typically be hotter than the shaft there should be no reduction of this fit at temperature. The stub shaft itself is hollow to reduce the transfer of heat from the disk to the bearings.

The disks were finished after assembly with the shaft by grinding on the shaft centers. In the case of similitude disks, the cone angle was machined onto the disk. The disks were then finish-lapped while mounted on their bearings, using a fine diamond dust compound with a special lapping fixture

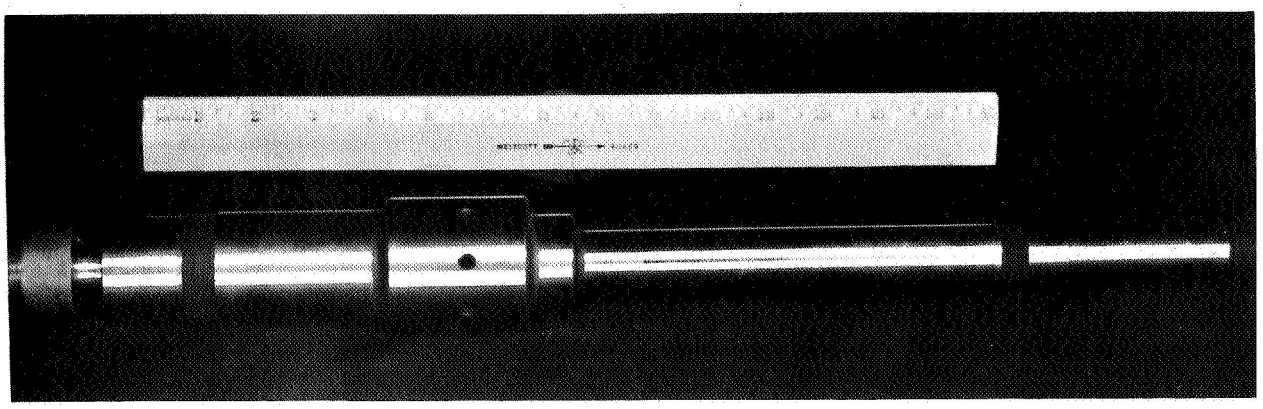

FIGURE 11. DRIVE SHAFT WITH INTEGRAL DISK

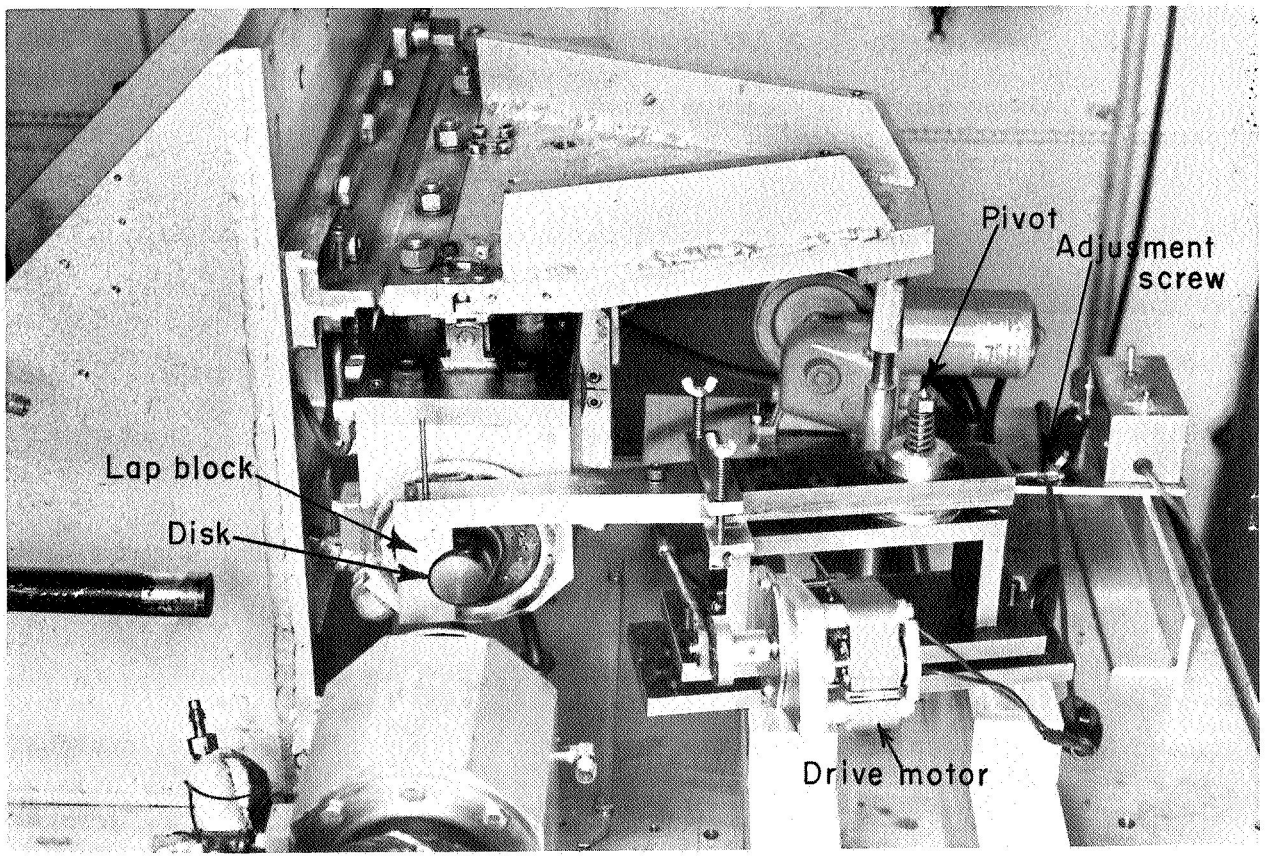

FIGURE 12. LAPPING FIXTURE IN OPERATION

designed to generate the crown radius. This fixture is shown in Figure 12 and involves a block-lap on an 11-in. swinging-arm arrangement. The resulting surface finish roughness was 1-2 microinches rms. The "run-out" of the disks after finish-lapping was approximately 50 x 10^{-6} in. TIR. A Talysurf trace of a replica of the finished lower disk is given in Figure 13. The disk-shaft assemblies were commercially balanced for speeds to 25,000 rpm.

Exploratory Experiments With Similitude Disks

Check-Out Tests

The target maximum conditions for the similitude-disk experiments were:

1. Disk speeds to 27,000 rpm to simulate bearings at 12,500 rpm
2. Loads producing bearing pressures to 400,000 psi
3. Temperatures to 600 F.

A preliminary check-out of the equipment revealed that the 600 F ambient temperature and the loading criteria were quite feasible. The upper limit on the speed of the disk, however, was limited by the drive motors to around 22,000 rpm.

Exploratory Experiments

Exploratory experiments have been conducted both to evaluate the usability of the apparatus and the film-thickness instrumentation plus the feasibility of disk film-thickness experiments for the target conditions. These experiments were conducted in a nitrogen environment with a synthetic paraffinic fluid, designated XRM-177, manufactured by Mobil Oil Company. Two types of experiments were conducted. One type involved measuring an axial profile of the lubricated contact zone between the disks using the X-ray technique. The second type of experiment involved

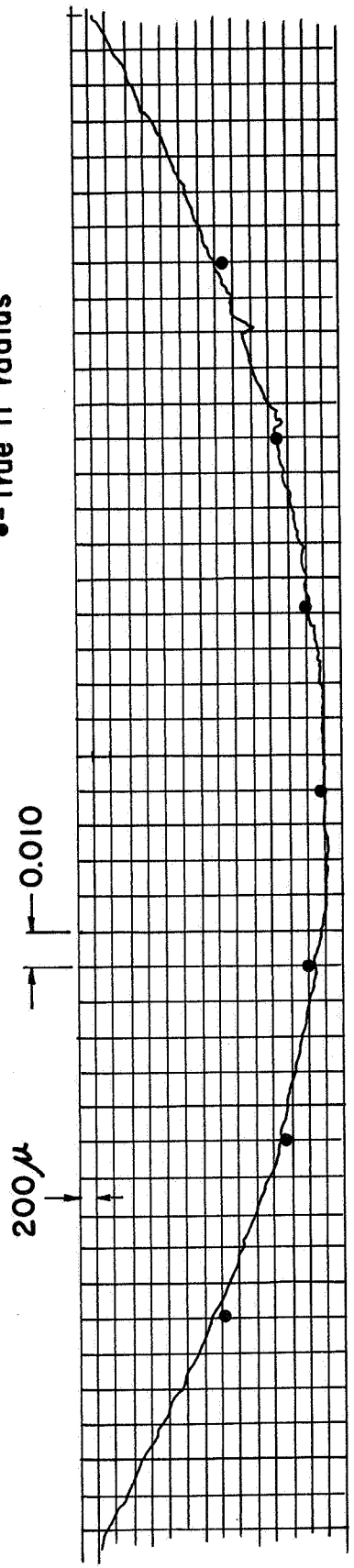

FIGURE 13. TALYSURF OF CONTOUR OF UPPER DISK

measuring only the minimum film thickness between the disks. A summary of the conditions included in the experiments is given in Table 4.

Experiments were successfully conducted at disk temperatures up to 600 F with the disk rotating at 20,000 rpm under 200,000 psi contact pressures. Under these very severe conditions only very thin films (~1 microinch) were observed using the X-ray technique. Further, partial although not complete breakdown of the lubricant film between the disk was observed at these conditions -- using the dielectric breakdown technique.

An axial profile of the disk contact zone obtained by scanning the X-ray counter, axially, in this zone is given in Figure 14 for a 600 F, 10,000 rpm, 200,000 psi condition. The mean film thickness indication here is about 1 microinch. The disks were adjusted tangentially such that the maximum X-ray signal was being received at the center of contact to ascertain that the disk contact zone was aligned with the X-ray beam. There appears to be a possible thinning of the film at the edges of the contact zone in this profile, although this edge thinning could also be due to a skewing of the upper disk relative to the lower. A later check of the disks revealed that apparent contact in the entire contact zone had occurred; evidence of scuffing in the edge regions was seen. A photograph taken of the upper disk after the experiments, showing the wear area and the scuffing is given in Figure 15.

At the 600 F, 10,000 rpm condition, the loading between the disks was increased to approximately 370, 000 psi to check the load-supporting capabilities of the lubricant. At this highest loading condition vibration in the apparatus occurred and indications of a zero film thickness were obtained, by the dielectric breakdown technique.

TABLE 4. SEQUENCE OF EXPLORATORY EXPERIMENTS WITH SIMILITUDE DISKS

Case Number	Temperature, F	Maximum Contact Pressure, psi	Speed, rpm	Type of Experiment	Minimum Film Thickness, microinches
1	Ambient	400,000	0		
2	200	200,000	10,000	Profile	18
3	"	250,000	10,000	"	15
4	"	200,000	15,000	Film Thickness	23
5	"	200,000	20,000	"	25
6	400	200,000	10,000	Profile	3
7	"	200,000	15,000	Film Thickness	4
8	"	200,000	20,000	"	6
9	600	200,000	10,000	Profile	~ 1
10	"	200,000	15,000	Film Thickness	~ 1
11	"	200,000	20,000	"	~ 1
12	"	250,000	20,000	"	~ 1
13	"	370,000	10,000	"	

(a) These disks were 1.41 in. in diameter and had a cone angle of 10 degrees.

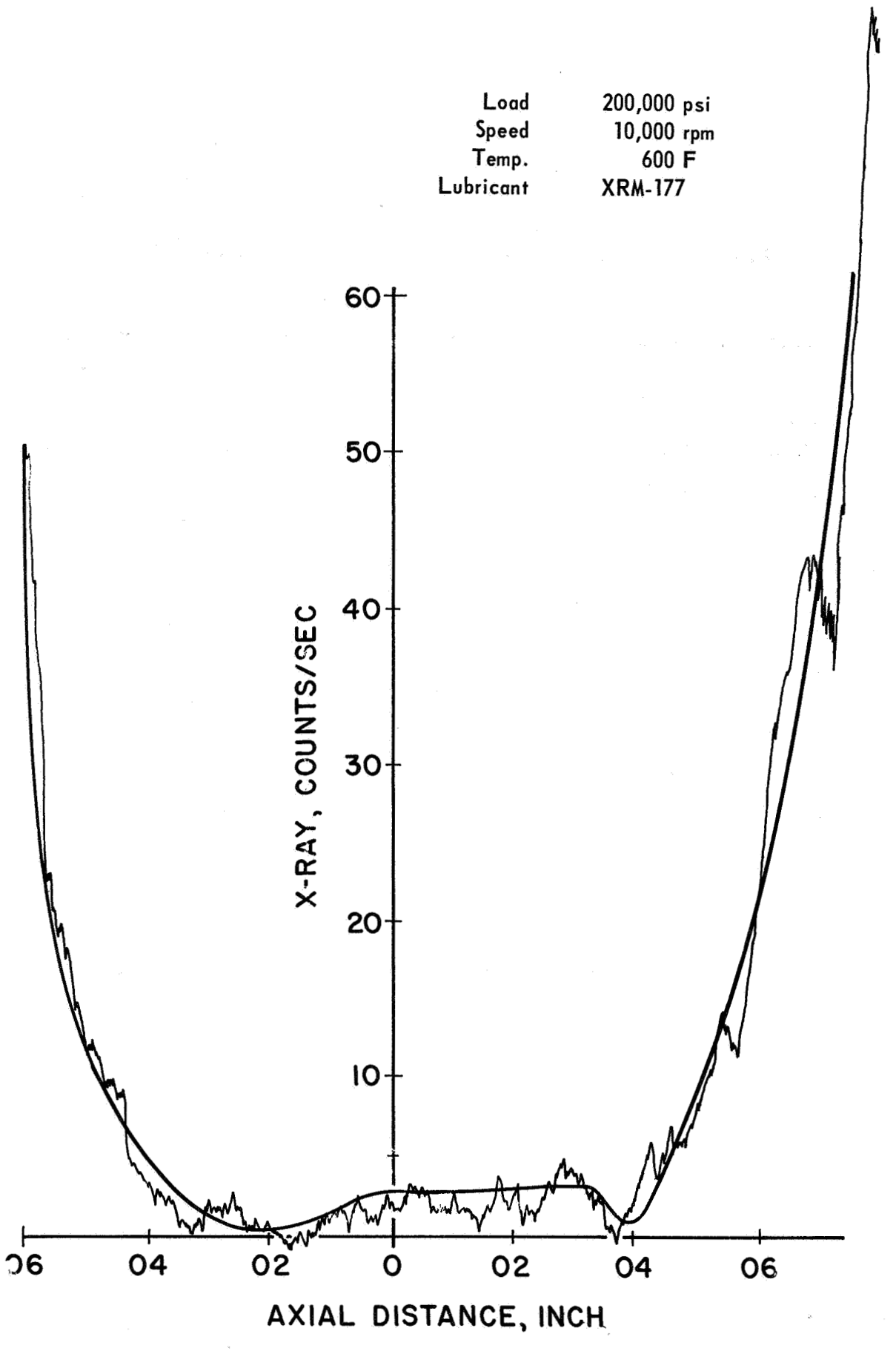

FIGURE 14. AXIAL PROFILE OF SIMILITUDE DISKS

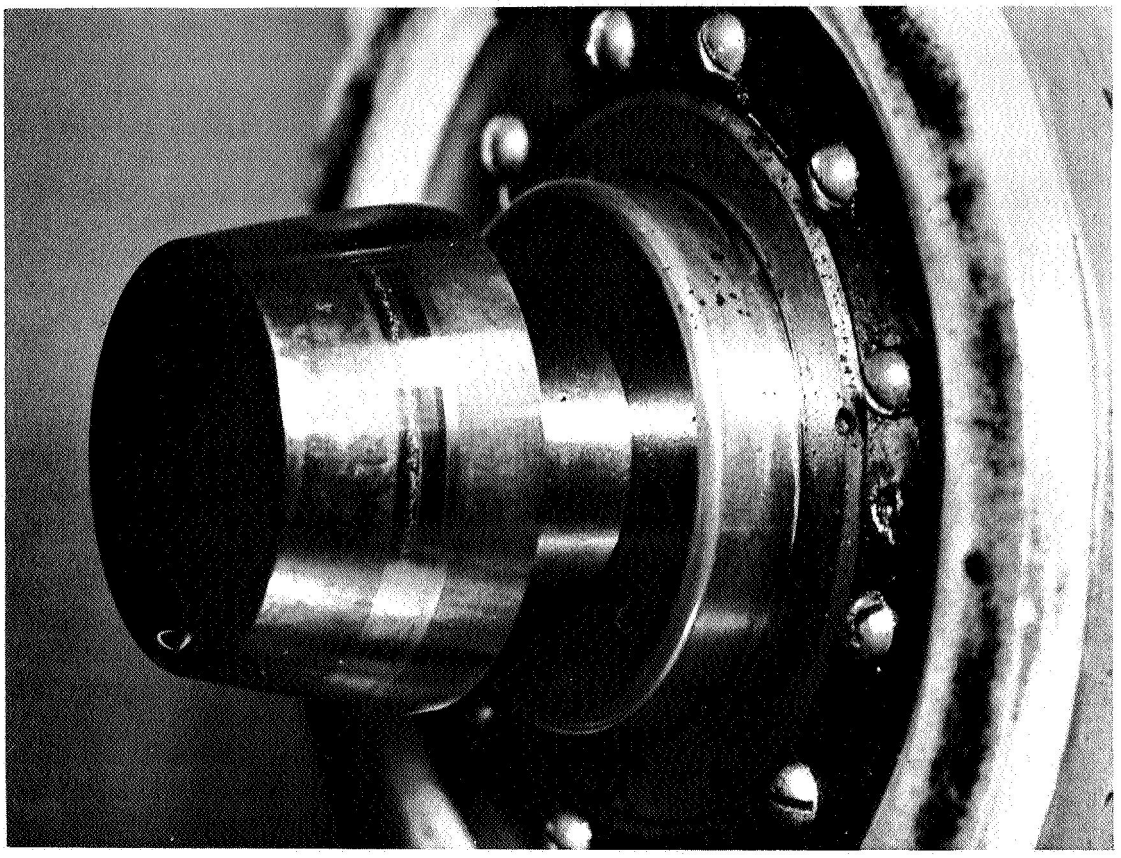

FIGURE 15. UPPER DISK AFTER RUNNING AT 200,000 PSI AND 600 F

At the lower temperature conditions a definite indication of a film was apparent for all of the few conditions checked. This film ranged from 3-4 microinches at 10,000 rpm to 5-6 microinches at 20,000 rpm for the 400 F conditions. Films of this magnitude are consistent with the extrapolation of other film thickness measurements obtained at Battelle. An axial profile obtained at 400 F for the 10,000-rpm, 200,000-psi condition is given in Figure 16. No apparent edge thinning exists in this profile. For the lowest temperature condition, 200 F, a sizable film was exhibited. An axial profile at this lower temperature condition is given in Figure 17.

In general the exploratory experiments have been quite informative about the lubrication of bearings under severe conditions of operation. However, these experiments were not intended as a mechanism for evaluating the XRM-177 lubricant or the feasibility of running bearings at 600 F, and much more elaborate experiments and observations are certainly needed. The results are intriguing and do demonstrate that this type of experiment is both possible and feasible. Future experiments should be most informative.

CONCLUSIONS

A program has been conducted to evaluate the feasibility of using an X-ray film thickness measuring scheme in conjunction with a lubricated rolling disk apparatus for evaluating lubrication under high load, high temperature and high speed conditions. The first objective of the study was to design a pair of disks that, when loaded together in lubricated contact, would yield an accurate simulation of the contact situation between a ball and race in a 120-mm-bore angular-contact bearing. The second objective was to evaluate the feasibility of conducting lubrication experiments with the designed disk under very severe conditions, using the X-ray techniques.

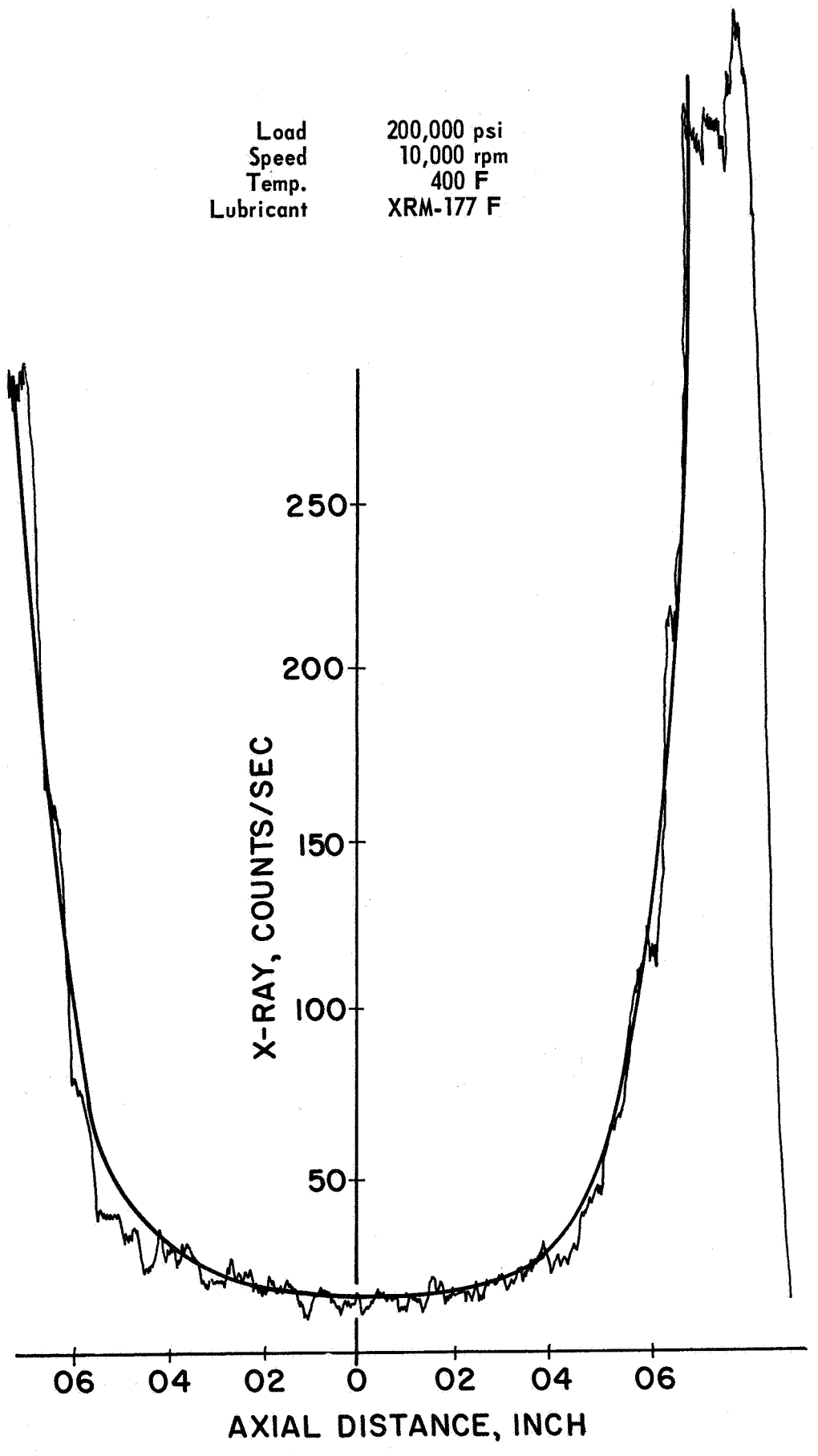

FIGURE 16. AXIAL PROFILE OF SIMILITUDE DISKS

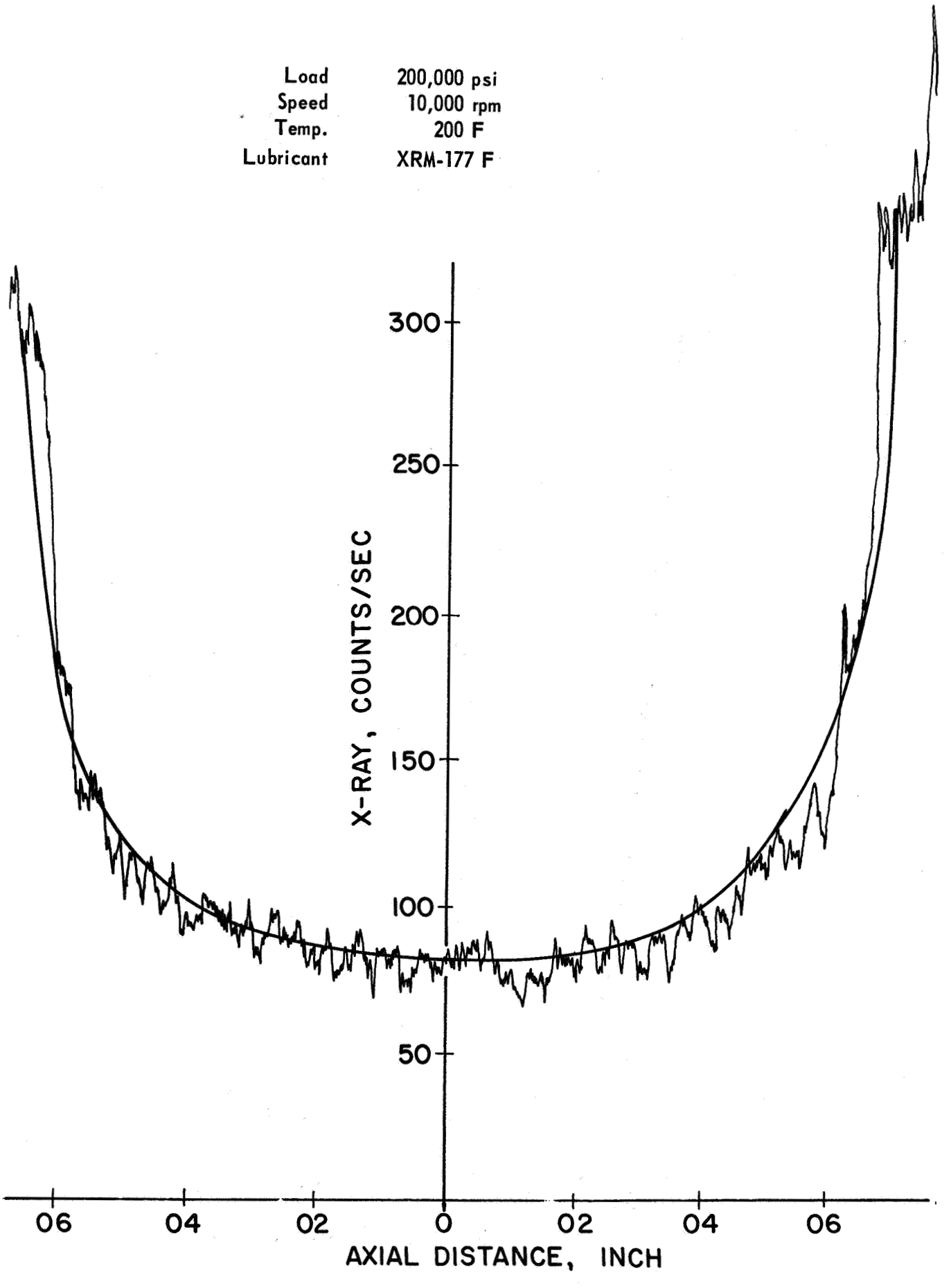

FIGURE 17. AXIAL PROFILE OF SIMILITUDE-DISKS

A comprehensive analysis was conducted in the study to define a disk geometry which would yield accurate simulation of a 120-mm-bore bearing. This analysis was based on a nondimensionalizing process for the differential equations governing bearing lubrication; consideration was given to elasticity effects, thermal effects, and hydrodynamic effects. As a result of this phase of the study it was concluded that accurate bearing lubrication experiments could be conducted with a pair of disks meeting the following specifications:

Disk Material	M-50 steel
Disk Diameter	1.42 in.
Cone Angle	10°
Tilt Angle	0°
Crown Radius	11 in.

Disk speeds to 27,000 rpm to simulate bearings at 12,500 rpm

Loads producing bearing pressures to 400,000 psi

Temperature 600 F.

An existing disk machine was modified to be used for the experiments. A set of disks meeting the target specifications was fabricated and lapped to a 1-2 microinch finish with almost perfect run-out in their support bearings. From a series of check-out experiments, it appears that all target conditions are feasible except perhaps the 27,000-rpm-speed conditions; here 20,000 rpm is the upper limit of the drive motors.

A series of exploratory experiments have been conducted to determine if measurable lubricant films exist under very severe condition of operation. At 600 F only very thin films were observed (~1 microinch) although there was

evidence of disk separation with both the X-ray technique and a dielectric breakdown scheme for a loading of even up to 200,000 psi contact pressure. At a temperature of 400 F a lubricant film around five microinches thick was observed.

In general, the study has shown that realistic simulation of bearing operation can be had using rolling disks, by suitable selection of the disk geometry. Further film-thickness experiments under high speed, high load, and high temperature appear to be quite feasible.

REFERENCES

(1) Sibley, L. B., and Austin, A. E., "An X-Ray Method For Measuring Thin Lubricant Films Between Rollers", ISA Trans., 3, 237-243 (1962).

(2) Kannel, J. W., Bell, J. C., and Allen, C. M., "Methods for Determining Pressure Distributions Between Lubricated Rolling Contacts", ASLE Trans., 8, pp 250-270 (1965).

(3) Rolling Element Computer Analysis Program (RECAP) calculations regarding NASA fatigue testers, included in letter from C. C. Moore of the General Electric Company, Cincinnati, Ohio, to C. M. Allen, dated April 15, 1965.

(4) RECAP calculations regarding NASA bearing, performed at General Electric Company, Cincinnati, Ohio, for C. C. Moore, with date unknown, but more recent than Reference 1.

(5) Bamberger, E. N., "Bearing Fatigue Investigation", Final Report on Contract NAS 3-7261, (September 15, 1967).

(6) Thomas, H. R., and Hoersch, V. A., "Stresses Due to the Pressure of One Elastic Solid Upon Another", University of Illinois Engineering Experiment Station Bulletin No. 212 (July, 1930).

(7) Dowson, D., Higginson, G. R., and Whitaker, A., "Elastohydrodynamic Lubrication: A Survey of Isothermal Solutions", J. Mech. Eng. Sci., 4, (2) pp 121-126 (1962).

(8) Dowson, D., and Whitaker, A. V. "A Numerical Prodedure for the Solution of the Elastohydrodynamic Problem of Rolling and Sliding Contacts Lubricated by a Newtonian Fluid", Inst. Mech. Engrs., Symposium on Elastohydrodynamic Lubrication, Leeds, Paper 4, pp 27-41 (September 21-23, 1965).

(9) Gohar, R., and Cameron, A., "The Mapping of Elastohydrodynamic Contacts", ASME Preprint No. 66 LC-21, presented at ASLE/ASME Lubrication Conference, Minneapolis (October 18-20, 1966).

(10) Cheng, H. S., "A Refined Solution to the Thermal-Elasto-Hydrodynamic Lubrication of Rolling and Sliding Cylinders, ASLE Preprint 65-AM-A42.

(11) Johnson, K. L., "A Review of the Theory of Rolling-Contact Stress", Wear, 9, pp 4-19 (1966).

(12) Pinkus, O., and Sternlicht, B., Theory of Hydrodynamic Lubrication, McGraw-Hill Book Co., Inc., New York (1961). (Cf. Eq. (1-10), p 12.)

(13) Timoshenko, S. P., Theory of Elasticity, McGraw-Hill Book Company, Inc., New York (1934). (See pp 344-349.)

(14) Bird, R. B., Stewart, E. W., and Lightfoot, E. N., Notes on Transport Phenomena, John Wiley and Sons, New York (1958). (Cf. the last equation on p. 187.)

APPENDIX

PRINCIPLES OF MODELING BALL-RACE LUBRICATION

APPENDIX

PRINCIPLES OF MODELING BALL-RACE LUBRICATION

Nature of the Problem

The shape of the lubricating film between a ball and its race and the distribution of pressure it exerts on the bearing surfaces depend on the physical properties of the surfaces and the lubricant and on operating conditions such as load, speed, and temperature. To get a good quantitative interpretation of these processes directly for a ball bearing, however, would require either experimentation which is still quite difficult or a laborious elastohydrodynamic analysis for which the foundations are still somewhat unstable.

Two disks rolling together in lubricated contact likewise develop a film of lubricant between them. Great similarity between this lubricating action and that generated by a ball rolling in a race could be had by making the conformity between the disks be the same as that between the ball and race, by imposing the same load and surface motions in both cases, and by using the same bearing materials, lubricant, and temperature. Such similarity might be advantageous for the study of lubrication in ball bearings, since it would allow experiments with disks to replace difficult experiments with ball bearings, but arranging thus for great similarity would bring difficult problems in itself. For example, the making of X-ray measurements of film-thickness requires the lubricating film to be flat enough to permit passage of X-rays. This flatness is impossible in most bearings, but it is not much less so in completely simulating disks. Again, if similarity is relaxed to allow geometric enlargement in order to facilitate use of a pressure transducer in the contact area between any experimental disks (here called the model) as compared to any bearing (here called the

prototype), then applying proper pressure over the larger area may overload the bearings supporting the disks as well as raise questions about loss of similarity through the enlargement. These sorts of problems demand an analysis of the similarity between the ball-bearing and experimental disk forms of lubrication. The analysis must allow for complexities such as toroidal rounding and spinning of the surfaces representing aspects of ball-race motion, and it should clarify the possible necessity of sacrificing some similarity in lubrication for experimental considerations.

One of the distinctive features of ball-race motion is that there is considerable variation of interfacial slip across the contact area. This slip arises because a ball typically spins with respect to one race as well as because the curvature of the contact area puts different parts of it at different distances from the axis of revolution of the ball. This latter component of slip, called Heathcote slip, varies parabolically from one side of the race to the other, whereas the slip due to ball spin varies almost linearly from side to side. Linear variation of slip from side to side can be simulated in the disk configuration by coning both disks, and parabolic variation can be had by making the rolling face concave on one disk and convex on the other. For the ball-race motion to be considered here, the slip contributed by ball spin is expected to be dominant, so coning of the disks is expected to be more important in the simulation process than is toroidal rounding. Nevertheless, both of these aspects of disk geometry will be given consideration.

A potentially important result of sliding between the ball and race surfaces is that the lubricant will undergo local heating, which of course can reduce the lubricant viscosity and hence alter the lubrication process. This indirect effect of ball-race slip (via temperature) can be more influential on

the lubrication processes than are the direct effects (that is, via forces arising directly from lubricant shearing).

Therefore, while some modeling of ball-race lubrication may be justifiable using a disk-disk configuration neglecting thermal aspects of the modeling process, really good modeling should include thermal as well as direct, mechanical similitude.

It will be shown that thermal similitude can be had in addition to mechanical similitude only under very restrictive conditions which may often be objectionably hard to fulfill. Therefore, consideration will be given first to isothermal modeling which treats thermal complications as being negligible, but attention will be given also to possible inclusion of thermal similitude.

In order to gain advantage from existing lubrication theories which treat almost exclusively the case of rolling cylinders, the problem of similitude between ball-race and disk-disk lubrication will be considered at first in terms of the theory for rolling cylinders, and the process will be assumed also to be isothermal. Then noncylindrical rollers will be considered, and thermal problems will be considered later. These considerations form the basis for modeling the particular ball-race configuration of the present study.

Notation

The notation to be used in the mathematical discussion includes the following:

c = specific heat of lubricant

E_1, E_2 = Young's modulus for material of surface No. 1, 2

$$E' = 1/\left[\frac{1-\nu_1^2}{\pi E_1} + \frac{1-\nu_2^2}{\pi E_2}\right]$$

h = distance between bearing surfaces = $h(x)$ or $h(x,y)$

h_o = value of h at film run-off position (outlet)

H = Rh/x_h^2 for cylindrical contact, $Rh/(x_h y_h)$ for elliptical contact

H_o = Rh_o/x_h^2 for cylindrical contact, $Rh_o/(x_u y_y)$ for elliptical contact

J = factor for converting thermal energy to mechanical energy

K = thermal conductivity of lubricant

m = $x_h/(R\Delta)$ = a tabulable function of R/R'

n = $y_h/(R\Delta)$ = a tabulable function of R/R'

p = pressure in lubricant = $p(x)$ or $p(x,y)$

p_h = maximum Hertz pressure

$P(\xi)$ = $p(x)/p_h$ = dimensionless pressure for cylindrical contact

$P(\xi,\eta)$ = $p(x,y)/p_h$ = dimensionless pressure for elliptical contact

R_1, R_2 = radius of curvature of surface No. 1, 2 in rolling direction

R_1', R_2' = radius of curvature of surface No. 1, 2 in axial direction (crown radius)

$$R = 1/\left(\frac{1}{R_1} + \frac{1}{R_2}\right), \quad R' = 1/\left(\frac{1}{R_1'} + \frac{1}{R_2'}\right)$$

$$S = \frac{\mu_o(u_1 + u_2)}{x_h p_h}\left(\frac{R}{x_h}\right)^2 = \text{a Sommerfeld number for cylindrical contact}$$

$$S_i = \frac{\mu_o(u_{1i} + u_{2i})}{p_h\sqrt{x_h y_h}}\,\frac{(x_h y_h)^{i/2} R^2}{x_h y_h} \text{ (for } i = 0,1,2) = \text{Sommerfeld numbers for elliptical contac}$$

T = $T(x,y,z)$ = absolute temperature in lubricant

u_i = surface velocity for surface No. i passing the contact area

= $u_{i0} + u_{i1}y + u_{i2}y^2$ for cases involving velocity variation in axial direction ($i = 1,2$)

u,v,w = lubricant velocity components in x, y, and z directions

W = load between bearing surfaces in elliptical contact

W' = load per unit length between bearing surfaces in cylindrical contact

x = distance in rolling direction (measured from coaxial plane)

x_h = half width of dry contact in rolling direction

x_o = value of x at runoff position of lubricant film (outlet)

y = distance in axial direction (measured from center plane)

y_h = half width of dry contact in axial direction for elliptical contact

z = distance from surface No. 1

α = pressure coefficient of density of lubricant

$\tilde{\alpha}$ = dimensionless maximum density exponent = αp_h

β = lubricant coefficient of thermal expansion (temperature coefficient of density)

γ = pressure coefficient of viscosity of lubricant

$\tilde{\gamma}$ = dimensionless maximum viscosity exponent = γp_h

$$\Delta = \sqrt[3]{\frac{3\pi WR'}{2E'R^2(R+R')}}$$

$\eta = y/\sqrt{x_h y_h}$ for elliptical contact

λ = ratio of R in experimental model to R in prototype bearing

μ = lubricant viscosity, assumed to be $\mu = \mu_o e^{\gamma p}$ for isothermal cases

μ_o = base viscosity of lubricant

ν_1,ν_2 = Poisson's ratio for material of surface No. 1, 2

ρ = lubricant density, assumed to be $\rho = \rho_o e^{\alpha p}$ for isothermal cases

$\xi = x/x_h$ for cylindrical contact, $x/\sqrt{x_h y_h}$ for elliptical contact

$\xi_o = x_o/x_h$ for cylindrical contact, or

$= \xi_o(\eta) = x_o(y)/\sqrt{x_h y_h}$ = dimensionless run-off position for lubricant in elliptical contact.

Isothermal Lubrication of Cylindrical Rollers

Loaded roller bearings deform in the region of contact, but the shape of the deformed surfaces depends somewhat on the hydrodynamic action of the lubricant. Complete mathematical description of the surface geometries and lubricant flow can be had only by solving the so-called elastohydrodynamic problem, which, unfortunately, is so complex that only solutions that have ever been published are numerical solutions referring to a few particular cases. [7,8,10] These solutions do provide some guidance of what lubricant film shapes and pressures may arise, so a generalized sketch of them is shown in Figure A-1 which also serves to illustrate some of the notation to be used here. For present purposes, however, particular elastohydrodynamic solutions are too restricted. What is needed is an overall look at the structure of the problem. Therefore, we shall consider instead the defining equations of the problem.

For rolling cylinders with an isothermal lubricant, the defining equations of the elastohydrodynamic problem include first the Reynolds equation relating lubricant pressure p to film thickness h at any position x:

$$\frac{dp}{dx} = 6\,\mu_o\,(u_1 + u_2)\,e^{\gamma p}\,\frac{h - h_o e^{-\alpha p}}{h^3} \quad . \tag{1}$$

Here, u_1 and u_2 are the velocities of the two surfaces passing the contact area, and it is assumed that the viscosity of the lubricant is $\mu = \mu_o e^{\gamma p}$ and its density is $\rho = \rho_o e^{\alpha p}$. The constant h_o can be interpreted as the film thickness at the runoff point (where $x = x_o$) since one usual boundary condition is that $\frac{dp}{dx} = 0$ at the runoff point. Next, there is the equation showing how the film shape arises from the original surface curvatures and the imposed deformations. This equation

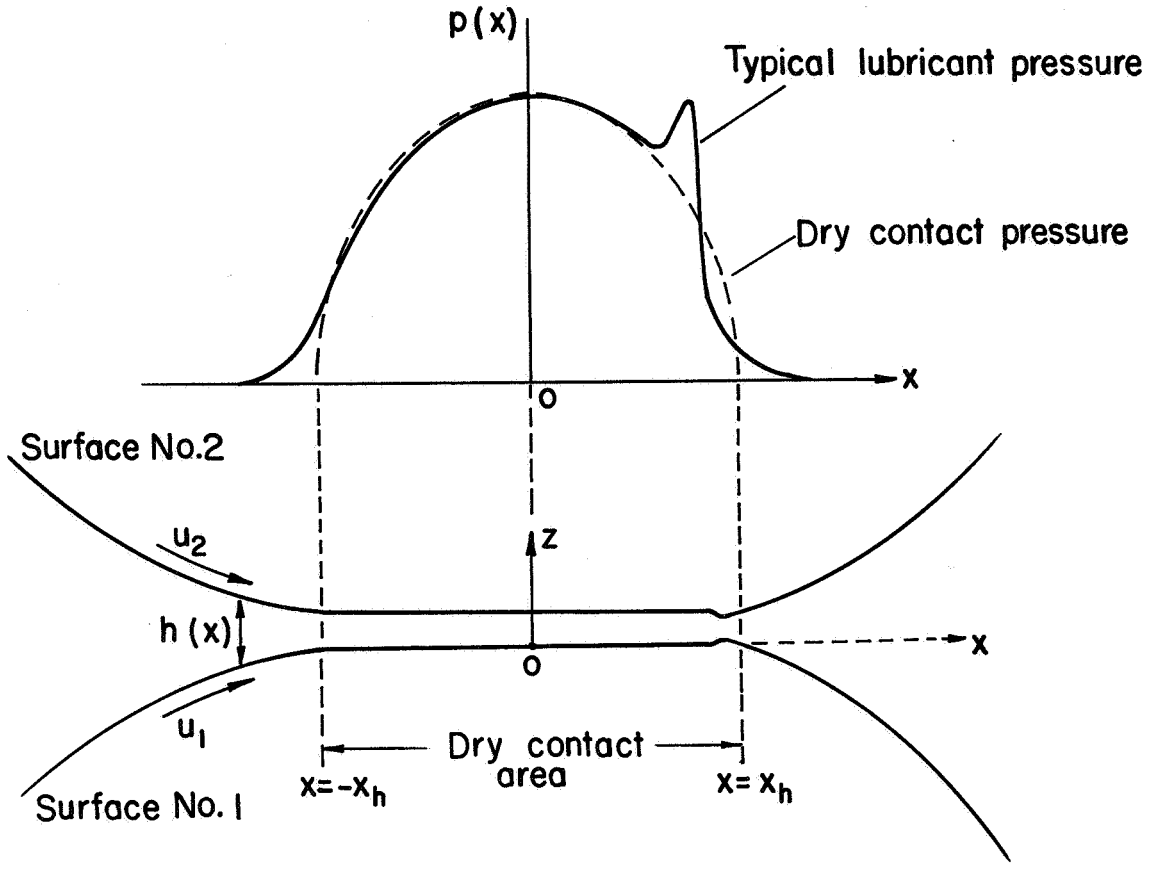

FIGURE AI. CONTACT GEOMETRY OF LUBRICATED, ROLLING CYLINDERS

may be written in the form*:

$$h(x) = h_o + \frac{1}{2R}(x^2 - x_o^2) - \frac{1}{E'}\int_{\infty}^{x_o} p(x') \ln \frac{|x - x'|}{|x_o - x'|}\, dx' \quad , \tag{2}$$

where

$$\frac{1}{R} = \frac{1}{R_1} + \frac{1}{R_2} \quad \text{and} \quad \frac{1}{E'} = \frac{1-\nu_1^2}{\pi E_1} + \frac{1-\nu_2^2}{\pi E_2} \quad ,$$

R_1 and R_2 being the radii of the two cylinders, E_1 and E_2 being their Young's moduli, and ν_1 and ν_2 being their Poisson ratios. Boundary conditions at inlet and outlet require that

$$p(-\infty) = p(x_o) = 0 \quad . \tag{3}$$

(Note that $\frac{dp}{dx} = 0$ at $x = x_o$ automatically in view of Equations (1) and (2).) In addition, the integral of the pressure over $-\infty < x \leq x_o$ must equal W', the load per unit axial length, that is

$$\int_{-\infty}^{x_o} p(x)\, dx = W' \quad . \tag{4}$$

Solution of the problem, including imposition of the three boundary conditions in Equations (3) and (4), would determine the functional forms of h(x) and p(x) and would fix the constants x_o, h_o, and the constant of integration implied by the differential Equation (1).

In order to make Equations (1), (2), (3), and (4) represent their elastohydrodynamic problem more compactly, dimensionless variables may be used. Thus let

$$\xi = \frac{x}{x_h} \quad , \quad H(\xi) = \frac{Rh(x)}{x_h^2} \quad , \quad P(\xi) = \frac{p(x)}{p_h} \quad , \quad \text{and} \quad \xi_o = \frac{x_o}{x_h} \quad ,$$

$$H_o = \frac{Rh_o}{x_h^2} \quad ,$$

---

* This equation is equivalent to Equation (1) in Reference 2.

where x_h is the half-width of the dry contact area, and p_h is the maximum dry-contact pressure. Then, recalling that

$$x_h = 2R\sqrt{\frac{W'}{E'R}} \quad \text{and} \quad p_h = \frac{E'}{\pi}\sqrt{\frac{W'}{E'R}} \ ,$$

the problem represented by Equations (1) through (4) can be rewritten as:

$$\left\{\begin{array}{ll} \dfrac{dP}{d\xi} = 6\,Se^{\tilde{\gamma}p}\,\dfrac{H-H_o e^{-\tilde{\alpha}P}}{H^3} \ , & (1') \\[2ex] H(\xi) = H_o + \dfrac{1}{2}(\xi^2-\xi_o^2) - \dfrac{1}{2\pi}\displaystyle\int_{-\infty}^{\xi_o} p(\xi')\,\ln\frac{|\xi-\xi'|}{|\xi_o-\xi'|}\,d\xi' \ , & (2') \\[2ex] P(-\infty) = P(\xi_o) = 0 \ , & (3') \\[2ex] \displaystyle\int_{-\infty}^{\xi_o} P(\xi)d\xi = \frac{\pi}{2} \ , & (4') \end{array}\right.$$

where

$$\left.\begin{array}{l} S = \dfrac{\mu_o(u_1+u_2)}{x_h p_h}\left(\dfrac{R}{x_h}\right)^2 = \dfrac{\pi\mu_o(u_1+u_2)}{8RE'}\left(\dfrac{E'R}{W'}\right)^2 \ , \\[2ex] \tilde{\alpha} = \alpha\, p_h = \dfrac{\alpha E'}{\pi}\sqrt{\dfrac{W'}{E'R}} \ , \\[2ex] \tilde{\gamma} = \gamma p_h = \dfrac{\gamma E'}{\pi}\sqrt{\dfrac{W'}{E'R}} \ . \end{array}\right\} \qquad (5)$$

These last three parameters are recognizable. S is a form of Sommerfeld number, $\tilde{\alpha}$ is the logarithm of the maximum density-variation factor, and $\tilde{\gamma}$ is the logarithm of the maximum viscosity-variation factor.* These are the three independent

* For the problem assuming an isothermal incompressible (α=0) lubricant, Dowson[7] introduced parameters he denoted as G, U, and W. Their relation to the present parameters is given by $S = (\pi^2/8)U/W^2$, $\tilde{\gamma}=(1/\sqrt{2\pi})GW^{1/2}$ and $(\pi/2)(x_h/2R)^2=W$. It is interesting to observe that Johnson[11], following Blok, has already observed that Dowson's parameters were not all needed for defining suitably dimensional pressure solutions and that U/W^2 and γp_h are convenient reduced parameters.

parameters that remain in the dimensionless form of the problem. (The values of H_o and ξ_o are determined through meeting the boundary conditions.) Therefore, the solution to the dimensionless problem must have the form

$$H \equiv H(S, \tilde{\alpha}, \tilde{\gamma}; \xi) \quad , \quad P \equiv P(S, \tilde{\alpha}, \tilde{\gamma}; \xi) \quad ,$$
$$\xi_o = \xi_o(S, \tilde{\alpha}, \tilde{\gamma}) \quad , \quad H_o = H_o(S, \tilde{\alpha}, \tilde{\gamma}) \quad . \tag{6}$$

Suppose that equations of the forms (1) through (4) could be used to describe the lubrication of both a cylindrical roller bearing and a disk-disk model of it. If both configurations were designed to have the same values of S, $\tilde{\alpha}$, and $\tilde{\gamma}$, then measuring values of $H(\xi)$ and/or $P(\xi)$ in the disk-disk model would provide, in effect, measurements of the same quantities in the bearing; that is, a known and usable similarity would exist between the forms of lubrication in these two bearing configurations. This is the kind of relationship that should exist if experiments with a rolling-disk machine are to be used to explore the nature of lubrication in a particular bearing. There may remain, however, some doubt about whether the parameters S, $\tilde{\alpha}$, and $\tilde{\gamma}$ are logically necessary (not all of Dowson's G, U, and W were), and whether some of them produce only negligible effects.

In order to judge the importance of the parameters S, $\tilde{\alpha}$, and $\tilde{\gamma}$, we may turn to the published numerical solutions of this kind of problem. Correlating the results of several calculations which presumed the lubricant to be incompressible ($\tilde{\alpha}$=0) as well as isothermal, Dowson[7] found in effect that the minimum value of H, which approximates H_o, is

$$H_{min} = 0.94\ S^{0.7}\ \tilde{\gamma}^{0.6} \quad .$$

Grubin, using further an assumed entrance-film shape in order to avoid complicated calculations, found in effect that

$$H_o = 1.28\ S^{\frac{8}{11}}\ \tilde{\gamma}^{\frac{8}{11}} \quad .$$

These formulas differ slightly in their predictions (Dowson's being generally

smaller, part of the difference being in the terminal dip which Grubin ignored), but in either case H_o is approximately proportional to $(S\tilde{\gamma})^{0.7}$. Thus, $S\tilde{\gamma}$ should be a significant parameter. Beyond this, Johnson [11] has remarked that the shape of Dowson's pressure solutions, while depending on both Dowson's parameter U/W^2 and the logarithm of the maximum pressure-variation factor (that is on both S and $\tilde{\gamma}$), depends mainly on Dowson's U/W^2 (that is, mainly on S). Thus, considering both film thickness and pressure effects, it is seen that both S and $\tilde{\gamma}$ are independently important parameters. Furthermore, in considering the effect of lubricant compressibility, Dowson [7] found that while including compressibility did not change the minimum film thickness very much, it did alter the height of the pressure spike drastically. To this extent, the value of $\tilde{\alpha}$ also is significant, though it must be admitted that the high pressure spike may always be far less important than shown by the analysis neglecting compressibility.

It is not contemplated that purely cylindrical disks should be used in the forthcoming experiments for the present research, but it is believed that the principles of simulation that have been illustrated and the importance ratings found for the various parameters will serve well as guidelines for more complex simulation processes.

Isothermal Lubrication of Rolling Surfaces Slipping Nonuniformly

The lubrication processes in the ball-race configuration differ significantly from those with rolling cylinders in that the contact area has finite axial length and that each surface velocity varies quadratically in the axial direction. Since these quadratic variations are unequal, there is also a quadratic axial variation of slip between the surfaces. These differences from the

cylindrical case are great enough to demand a fresh evaluation of the requirements for similarity between a bearing and a rolling disk model of it.

Full consideration of similarity between these configurations would require inclusion of thermal effects, since slipping of the bearing surfaces may produce its major effects by way of the heat it generates. Thermal simulation, however, involves so many additions to the simulation problem that it is reasonable to ignore it temporarily and to explore what can be done with similarity when the thermal influences are negligible, so this will be done.

Let it be supposed now that two surfaces roll together having a contact area which is finitely long in the axial direction and having velocities u_1 and u_2 that vary quadratically in that direction. Such a contact region is shown schematically in Figure A-2. The axes shown there put the origin where the center of dry contact would be on one surface, and the x and y axes lie in that surface. (While viewing Figure A-2, it should be observed that the variation of surface velocity according to axial position is not associated with shearing of the surfaces; it arises instead from tilting of the y-axis with respect to the axes of revolution, including bending of the y-axis as it conforms to an actual bearing surface.) Thus, it is assumed that

$$u_1 = u_{10} + u_{11}\, y + u_{12}\, y^2 \quad ,$$
$$u_2 = u_{20} + u_{21}\, y + u_{22}\, y^2 \quad . \tag{9}$$

Despite this variation of u_1 and u_2, a rederivation of the Reynolds equation for two-dimensional lubricant flow shows that the equation still has the accustomed two-dimensional form[12] which may be written as

$$\frac{\partial}{\partial x}\left[e^{(\alpha-\gamma)p}\, h^3\, \frac{\partial p}{\partial x}\right] + \frac{\partial}{\partial y}\left[e^{(\alpha-\gamma)p}\, h^3\, \frac{\partial p}{\partial y}\right] = 6\, \mu_o (u_1 + u_2)\, \frac{\partial}{\partial x}\left(e^{\alpha p} h\right) \quad , \tag{10}$$

where again p is pressure, lubricant viscosity is $\mu = \mu_o e^{\gamma p}$, and lubricant density

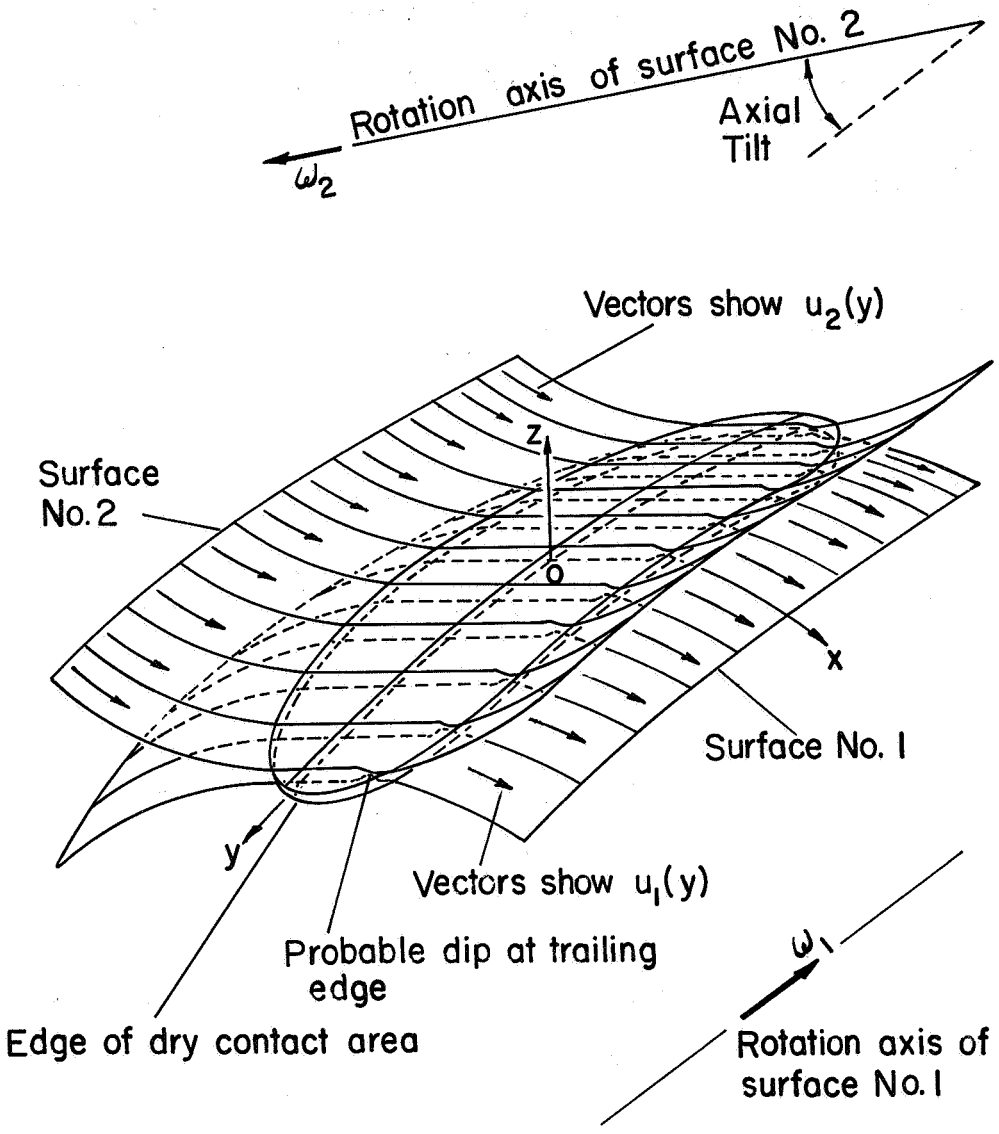

FIGURE A2. CONTACT GEOMETRY OF LUBRICATED CROWNED, ROLLING SURFACES WITH TILTED AXES OF ROTATION

is $\rho = \rho_o e^{\alpha p}$. If the principal curvatures of the surfaces at the origin are R_1 and R_2 in the x-direction, and R_1' and R_2' in the y-direction, then apart from surface deformation the separation of dry, contacting surfaces would be

$$\frac{x^2}{2R} + \frac{y^2}{2R'} \quad ,$$

where

$$\frac{1}{R} = \frac{1}{R_1} + \frac{1}{R_2} \quad , \qquad \frac{1}{R'} = \frac{1}{R_1'} + \frac{1}{R_2'} \quad .$$

Accounting for surface deformation[13] and the surface separation at the origin, the surface separation at an arbitrary point can be written

$$h(x,y) = h(0,0) + \frac{x^2}{2R} + \frac{y^2}{2R'} + \frac{1}{E'} \iint \frac{p(x',y')dx'dy'}{\sqrt{(x-x')^2 + (y-y')^2}} - \frac{1}{E'} \iint \frac{p(x',y')dx'dy'}{\sqrt{x'^2 + y'^2}} \quad , \tag{11}$$

where the integrals are taken over the entire pressure region, and again

$$\frac{1}{E'} = \frac{1-\nu_1^2}{\pi E_1} + \frac{1-\nu_2^2}{\pi E_2} \quad .$$

Equations (10) and (11) provide determining equations for the functions $h(x,y)$ and $p(x,y)$ subject to the boundary conditions

$$p_{inlet} = p(x_o,y) = \left(\frac{dp}{dx}\right)_{x=x_o} = 0 \quad , \tag{12}$$

$$\iint p(x,y)\, dx\, dy = W \quad , \tag{13}$$

where $x_o(y)$ denotes the runoff position, W denotes the total load on the bearing surfaces, and the integral is taken over the entire pressure area. Solving the system of Equations (10), (11), (12), and (13) would produce not only the functions $h(x,y)$ and $p(x,y)$ but also a runoff position function $x_o(y)$ and a center film thickness $h(0,0)$.

In order to reduce this system of equations to dimensionless form, choice must be made of reference lengths and pressure. Guidance concerning these choices can be had from the Hertz theory for dry contact, which shows that x_h and y_h (the semiaxes of the contact ellipse) and p_h (the maximum pressure) are

$$x_h = mR\Delta, \quad y_h = nR\Delta, \quad p_h = \frac{E'\Delta}{\pi^2 m\, n}\left(1 + \frac{R}{R'}\right) \quad , \tag{14}$$

where

$$\Delta = \sqrt[3]{\frac{3\pi WR'}{2E'R^2(R+R')}} \quad .$$

and m and n are functions of R/R'.[13] (The values of m and n also change if the principal directions of curvature differ between the two surfaces, but no difference in these directions needs to be considered here.) It is desirable for present purposes that the same reference length should be chosen in both the x- and y-directions. A convenient choice for that reference length turns out to be $\sqrt{x_h y_h}$. Thus, we introduce the dimensionless variables

$$\xi = \frac{x}{\sqrt{x_h y_h}} \quad , \quad \eta = \frac{y}{\sqrt{x_h y_h}} \quad , \quad H(\xi,\eta) = \frac{Rh(x,y)}{x_h y_h} \quad , \quad p(\xi,\eta) = \frac{p(x,y)}{p_h} \tag{15}$$

and the dimensionless parameters

$$\tilde{\alpha} = \alpha\, p_h \quad , \quad \tilde{\gamma} = \tilde{\gamma}\, p_h \quad , \text{ and}$$

$$S_i = \frac{\mu_o(u_{1i} + u_{2i})}{p_h\sqrt{x_h y_h}} \cdot \frac{(x_h y_h)^{i/2} R^2}{x_h y_h} \quad , \quad \text{for } i = 0,1,2. \tag{16}$$

Then, Equations (10), (11), (12), and (13) take the forms

$$\frac{\partial}{\partial\xi}\left[e^{(\tilde{\alpha}-\tilde{\gamma})P}\,H^3\,\frac{\partial P}{\partial\xi}\right]+\frac{\partial}{\partial\eta}\left[e^{(\tilde{\alpha}-\tilde{\gamma})P}\,H^3\,\frac{\partial P}{\partial\eta}\right]=6(S_o+S_1\eta+S_2\eta^2)\,\frac{\partial}{\partial\xi}\,(e^{\tilde{\alpha}P}H), \quad (10')$$

$$H(\xi,\eta)=H(0,0)+\frac{1}{2}\left(\xi^2+\frac{R}{R'}\eta^2\right)+\frac{1}{\pi^2(m\,n)^{3/2}}\left(1+\frac{R}{R'}\right)\left[\iint\frac{P(\xi',\eta')d\xi'd\eta'}{\sqrt{(\xi-\xi')^2+(\eta-\eta')^2}}\right.$$
$$\left.-\iint\frac{P(\xi',\eta')d\xi'd\eta'}{\sqrt{\xi'^2+\eta'^2}}\right], \quad (11')$$

$$P_{inlet}=P(\xi_o,\eta)=\left(\frac{dP}{d\xi}\right)_{\xi=\xi_o}=0, \quad (12')$$

$$\iint P(\xi,\eta)d\xi d\eta=\frac{2\pi}{3}, \quad (13')$$

where

$$\xi_o(\eta)=x_o(y)/\sqrt{x_h y_h}.$$

This system of equations determining $H(\xi,\eta)$ and $P(\xi,\eta)$ involves the parameters $\tilde{\alpha}$, $\tilde{\gamma}$, $\frac{R}{R'}$, S_o, S_1, and S_2. If those parameters are assigned, then we should expect (according to this formulation of the problem) that $H(\xi,\eta)$ and $P(\xi,\eta)$ are thereby uniquely determined, and that $\xi_o(\eta)$ and $H(0,0)$ are determined also, since this is analogous to what is known about the case with cylindrical rollers. Thus, if a disk-disk configuration can be constructed and operated keeping these six parameters the same as for a certain ball-race configuration, then $H(\xi,\eta)$ and $P(\xi,\eta)$ should be the same for both configurations, and measurements of h or p in the disk-disk configuration should provide in effect measurements of h and p for the ball-race configuration. An exception to this similitude can arise, of course, if thermal disturbances in the contact area affect h or p significantly.

There may be doubt about whether all six of these parameters ($\tilde{\alpha}$, $\tilde{\gamma}$, $\frac{R}{R'}$, S_o, S_1, S_2) must be kept constant in passing from a ball-race prototype bearing to a disk-disk model of it, since the effect of some of them might be insignificant. This issue can be judged partly by referring back to the cylindrical-roller theory, which is a sort of limiting case of the ball-race

theory for $R/R' \to 0$. The parameters $\tilde{\alpha}$, $\tilde{\gamma}$, and S, which occurred and were significant there, are closely related to the present $\tilde{\alpha}$, $\tilde{\gamma}$, and S_o, so these three should affect $H(\xi,\eta)$ and/or $P(\xi,\eta)$ significantly. The characteristic three-dimensional aspects of the ball-race configuration are defined by the parameters R/R', S_1, and S_2 so insofar as a disk-disk experiment is intended to represent a ball bearing those parameters are significant too. The parameter R/R' may be regarded as relating to conditions near the ends of contact in the axial direction, S_1 relates primarily to the effects of ball spin, and S_2 relates to parabolic velocity variations like those of Heathcote slip.

It should be observed that if the same bearing metals and lubricant are used in the disk-disk experiment as in the prototype ball bearing, and if $\frac{R}{R'}$ and $\tilde{\gamma}$ are preserved in passing from the prototype to the experiment as they should be, then Δ also must be preserved. The geometrical scales in the x and y directions in the contact area, however, will change by the same factor as is applied to R, the relative radius of rolling curvature, since $x = \xi R\Delta\sqrt{mn}$ and $y = \eta R\Delta\sqrt{mn}$. The same geometrical factor also will be applied automatically to the film thickness, h, since $h = HmnR\Delta^2$. The pressure, p, will not be altered, though in accomplishing this the load, W, and velocity components must be scaled properly to keep Δ, S_o, S_1, and S_2 fixed. For example, in proper modeling using the same bearing materials and lubricant, the doubling of R in the experiment as compared to the model would require also the doubling of $u_{10} + u_{20}$, duplication of $u_{11} + u_{21}$, halving of $u_{12} + u_{22}$, and quadrupling of W. This change would result in the doubling of x_h, y_h, and $h(x,y)$, though $p(x,y)$ would not be altered.

Effects of Local Thermal Disturbances

The surface velocities u_1 and u_2 enter the mathematical problem for isothermal lubrication of a ball-race configuration only by way of the Reynolds

equation (10), and there only the sum $u_1 + u_2$ appears. Thus, slipping between the surfaces (that is $u_1 - u_2$) is of no consequence if the lubrication is isothermal in the manner that was presumed. It is known, of course, that lubricant viscosity is sensitive to temperature changes, and surface slipping appears quite apt to induce temperature changes. Therefore, it is desirable to pursue the effect of temperature changes that may result from representing a ball-race configuration by a pair of rolling disks.

A study of modeling including thermal effects in their entirety would require a complete rederivation of the Reynolds equation, and would show that equation to be considerably altered. The revised equation would involve also the temperature distribution $T(x,y,z)$ and its application would show $T(x,y,z)$ should be alike in the bearing and the experiment. In order to determine $T(x,y,z)$, here taken to be absolute temperature, it would be necessary to add to the mathematical problem the thermal energy equation plus several new boundary conditions. The thermal energy equation can be shown to have the form*

$$J\rho c\left(u\frac{\partial T}{\partial x}+v\frac{\partial T}{\partial y}+w\frac{\partial T}{\partial z}\right)-JK\frac{\partial^2 T}{\partial z^2}=\mu\left[\left(\frac{\partial u}{\partial z}\right)^2+\left(\frac{\partial v}{\partial z}\right)^2\right]+\beta T\left(u\frac{\partial p}{\partial x}+v\frac{\partial p}{\partial y}\right) \quad . \qquad (17)$$

The added notation here includes u, v, and w which are the three components of lubricant velocity in the x-, y-, and z-directions at any point, the thermal conductivity K and specific heat, c, of the lubricant, its density, ρ, and its coefficient of thermal expansion, β, and the factor J for converting thermal energy to mechanical energy. Suitable boundary conditions can be added also, but the energy equation itself provides sufficient challenge for the present.

If the relative radius of rolling curvature is multiplied by some factor λ in passing from the ball-race to disk-disk configuration and unaltered

---

* This is a special form of the last equation on p 187 of Reference 14.

bearing materials and lubricants are used, then consistency with the demands of isothermal modeling (which is a special case of thermal modeling) implies that x, y, and z as actual distances will change by the same factor λ, and that u will also change by this factor. A ready extension of these results is that v and w also can be expected to change by this factor λ, though $p(x,y)$ and $T(x,y,z)$ should not change. Using unaltered materials implies, of course, that K, ρ, c, β, and μ should not change. Accounting for how the factor λ would alter the several terms of Equation (17), one can see that all the introductions of the factor λ cancel each other except in the term $JK \frac{\partial^2 T}{\partial z^2}$ where a factor λ^2 remains uncancelled. To keep this term unchanged (that is in proper relation to the other terms of the equation), one would like to multiply the thermal conductivity K by λ^2 in passing from the prototype bearing to the experimental model of it, but this is not feasible if $\lambda \neq 1$. Thus, in order to achieve proper thermal modeling we are forced to take $\lambda = 1$, that is to make no change in R, the relative radius of rolling curvature. We can see that if we do change R, then the configuration with the larger R will also have the larger thermal disturbances, since its lack of an enlarged K will cause slower heat dissipation. If we were to consider also the new boundary conditions, we would find there also a necessity for increasing the thermal conductivities of the bearing materials if we were to take $\lambda > 1$.

The essence of these remarks is that if local temperature changes have any significant effect on quantities such as $h(x,y)$ or $p(x,y)$ which might be measured in the experimental model, then those measurements will be distorted if any change is made in the relative radius of rolling curvature as we pass from the prototype bearing to the experimental model. If local temperature changes are insignificant in both the prototype and the model of it, then it is

acceptable to change this radius provided the proper corresponding changes are made in the total rolling velocity and the load as was described under isothermal modeling.

Systematic study of thermal similitude shows further (even before one puts $\lambda = 1$) that in modeling without change of bearing material or lubricant one should preserve $[u_2(y) - u_1(y)]/R$ as well as $[u_1(y) + u_2(y)]/R$. A direct consequence then is that both $u_1(y)/R$ and $u_2(y)/R$ should be preserved.

Modeling which introduces changes of bearing materials or lubricants obviously introduces further possibilities, but these seem to have mainly academic interest for the present research since it is expected to be tied closely to predetermined choices of materials which can not well be altered.

TASK II FINAL - REPORT CR 72346
CONTRACT NAS3-7270

DISTRIBUTION LIST

NASA Headquarters
Washington, D. C. 20546
Attention: N. F. Rekos (RAP)
M. Comberiate

NASA-Lewis Research Center
21000 Brookpark Road
Cleveland, Ohio 44135
Attention: John H. DeFord, M.S. 60-5
Technology Utilization Office, M.S. 3-19
P. T. Hacker, M.S. 5-3
I. I. Pinkel, M.S. 5-3
J. Howard Childs, M.S. 60-4 (2 copies)
D. Townsend, M.S. 60-4 (4 copies)
L. Macioce, M.S. 60-4
E. E. Bisson, M.S. 5-3
R. L. Johnson, M.S. 23-2
W. J. Anderson, M.S. 23-2
E. V. Zaretsky, M.S. 6-1 (12 copies)
Reports Control Office, M.S. 5-5

FAA Headquarters
800 Independence Avenue, S.W.
Washington, D. C. 20553
Attention: F. B. Howard/SS-120
Brig. General J. C. Maxwell

Air Force Materials Laboratory
Wright-Patterson AFB, Ohio 45433
Attention: MANL
R. Adamczak & F. Harsacky
MAMD
Walter Trapp

NASA-Langley Research Center
Langley Station
Hampton, Virginia 23365
Attention: Mark R. Nichols

United Aircraft Corporation
Pratt & Whitney Aircraft Division
East Hartford, Connecticut 06108
Attention: R. P. Schevchenko
P. Brown

General Electric Company
Gas Turbine Division
Evendale, Ohio 45215
Attention: B. Venable
E. N. Bamberger

California Research Corporation
Richmond, California 94802
Attention: Douglas Godfrey

Dow Chemical Company
Abbott Road Buildings
Midland, Michigan 48640
Attention: Dr. R. Gunderson

Crucible Steel Company of America
The Oliver Building
Mellon Square
Pittsburgh, Pennsylvania 15222

Dow Corning Corporation
Midland, Michigan 48640
Attention: R. W. Awe & H. M. Schiefer

Allegheny Ludlum Steel Corporation
Oliver Building
Pittsburgh, Pennsylvania 15222

Mechanical Technology, Incorporated
Latham, New York 14603
Attention: B. Sternlicht

Director
Government Research Laboratory
Esso Research & Engineering Company
P.O. Box 8
Linden, New Jersey 07036

Industrial Tectonics, Inc.
Research & Development Division
18301 Santa Fe Avenue
Compton, California 90220
Attention: Heinz Hanau

Monsanto Research Corporation
Everett Station
Boston, Massachusetts 02109
Attention: Dr. John O. Smith

Pennsylvania State University
Department of Chemical Engineering
University Park, Pennsylvania 16801
Attention: Dr. E. E. Klause

Fafnir Bearing Company
37 Booth Street
New Britain, Connecticut 06051
Attention: H. B. Van Dorn

General Electric Company
General Engineering Laboratory
Schenectady, New York 12305

DISTRIBUTION LIST (Continued)

Borg-Warner Corporation
Roy C. Ingersoll Research Center
Wolf and Algonquin Roads
Des Plaines, Illinois 60016

General Motors Corporation
New Departure Division
Bristol, Connecticut 06010
Attention: W. O'Rourke

Franklin Institute Labs
20th and Parkway
Philadelphia, Pennsylvania 19133
Attention: Otto Decker

Westinghouse Electric Corporation
Research Laboratories
Beulah Road, Churchill Borough
Pittsburgh, Pennsylvania 15235
Attention: John Boyd

Midwest Research Institute
425 Volker Boulevard
Kansas City, Missouri 64110
Attention: V. Hopkins & A. D. St. John

Socony Mobil Oil Company
Research Department
Paulsboro Laboratory
Paulsboro, New Jersey 08066
Attention: Ed. Oberright

The Marlin-Rockwell Corporation
Jamestown, New York 14701
Attention: Arthur S. Irwin

Southwest Research Institute
San Antonio, Texas 78205
Attention: P. M. Ku

IIT Research Institute
West 35th Street
Chicago, Illinois 60616
Attention: Warren Jamison

NASA-Lewis Research Center
21000 Brookpark Road
Cleveland, Ohio 44135
Attention: Library

Sinclair Research, Incorporated
400 E. Sibley Boulevard
Harvey, Illinois 60426
Attention: M. R. Fairlie
Director of Products Division

NASA-Scientific and Technical Information Facility
Box 5700
College Park, Maryland 20740
Attention: NASA Representative (6 copies)

AiResearch Manufacturing Company
Dept. 93-3
9851 Sepulveda Boulevard
Los Angeles, California 90009
Attention: Hans. J. Poulsen

Department of the Army
U. S. Army Aviation Material Labs.
Fort Eustis, Virginia 23604
Attention: J. W. White
Propulsion Division

SKF Industries, Inc.
Engineering & Research Center
1100 First Avenue
King of Prussia, Pennsylvania 19104
Attention: L. B. Sibley
T. Tallian

Hyatt Division
New Departure Bearing Company
Sandusky, Ohio 44870
Attention: B. Ruley

Timkin Roller Bearing Company
Canton, Ohio 44701
Attention: Dr. W. Littmann

Caterpillar Tractor
Peoria, Illinois 61601
Attention: B. Kelley

General Motors Research Laboratory
Warren, Michigan 48089
Attention: Nils L. Buench

Department of the Navy
Naval Ship Research
Development Center
Annapolis, Maryland 21402
Attention: Paul Schatzberg

Plasmadyne
3839 South Main Street
Santa Ana, California 92702
Attention: J. W. Rosenbery

Westinghouse Electric Corporation
Small Steam & Gas Turbine Engrg. B-4
Lester Branch, P.O. Box 9175
Philadelphia, Pennsylvania 19113
Attention: S. M. DeCorso